

# Theory of non-Markovian relaxation of single triplet electron spins using time- and frequency-domain magnetic resonance spectroscopy measured via optical fluorescence: Application to single pentacene molecules in crystalline *p*-terphenyl

S. Ya. Kilin and A. P. Nizovtsev

*Institute of Physics Academy of Sciences of Belarus, F. Skarina Avenue 70, Minsk, 220602, Belarus*

P. R. Berman

*University of Michigan, Ann Arbor, Michigan 48109-1120*

C. von Borczyskowski and J. Wrachtrup

*Institute of Physics, Technical University of Chemnitz, D-09107, Chemnitz, Germany*

(Received 24 December 1997)

Fluorescence-detected magnetic resonance (FDMR) allows one to monitor magnetic resonance phenomena via fluorescence. Experimental FDMR data obtained using single triplet-state chromophore guest molecules in a low-temperature organic host matrix are analyzed using a stochastic approach to describe triplet electron spin dephasing resulting from frequency fluctuations  $U^t$  induced by host-matrix proton spin dynamics. Modeling the fluctuations  $U^t$  by a sum of  $N$  independent random telegraph processes with the same jump rate  $\nu$  but different variances  $\sigma_k$  we construct an exact set of equations for the density matrix of a five-level molecule averaged over fluctuation histories  $U^t$ . These equations provide a basis to study non-Markovian effects of microwave- (MW-) field-dependent dephasing in the FDMR response of a molecule undergoing slow fluctuations  $U^t$  ( $\sigma^2/\nu^2 \geq 1$ ,  $\sigma^2 = \sum \sigma_k^2$ ) to a MW field that is resonant with a transition between triplet spin substates. Both frequency- and time-domain FDMR phenomena such as (i) power-broadened FDMR line shapes, (ii) FDMR Hahn echo signals, and (iii) FDMR free induction decay are studied. Analytical expressions for the FDMR response are obtained in the case  $\nu \gg k_j^i$  where  $k_j^i$  is an intersystem crossing rate. Experimental data on power-broadened line shapes for a pentacene-*p*-terphenyl pair which demonstrate a pronounced effect of MW-field-suppressed dephasing are explained in the context of the theory. [S0163-1829(98)00337-3]

## I. INTRODUCTION

Since the first pioneering observations of absorption<sup>1</sup> and fluorescence<sup>2,3</sup> spectra of single chromophore molecules embedded in low-temperature host matrices, a variety of experimental methods have been applied to uncover different kinds of behavior of individual guest molecules in solids which are usually hidden by conventional ensemble averaging. Inherently single-molecule phenomena such as spectral diffusion,<sup>4-6</sup> photon bunching,<sup>2,7</sup> and antibunching<sup>8</sup> have been observed. Additionally, a new field of condensed matter spectroscopy, single molecular spectroscopy (SMS), has been advanced and developed. Using sensitive techniques one can now measure the distribution of spectroscopic parameters associated with different individual molecules. Moreover, it is possible to study the interactions of a single molecule with its nanoscopic local environment and to uncover the dynamics of various processes occurring in the neighborhood of the molecule (see, e.g., for a review Refs. 9 and 10 and the recent book in Ref. 11).

Of increasing importance in SMS is fluorescence-detected magnetic resonance (FDMR), where one observes changes in the fluorescence intensity of an optically excited individual molecule that occur when the molecule interacts with a cw/pulsed microwave (MW) field that resonantly drives transitions between molecular triplet electron spin substates. It has been demonstrated in Refs. 12-22 that this combination of SMS and electron paramagnetic resonance (EPR) methods is

very useful for obtaining a wealth of information about single triplet electron spins. Observations of FDMR line shapes,<sup>12,13</sup> of the influence of microwaves on the fluorescence intensity correlation function  $g^{(2)}(\tau)$ ,<sup>7,15,18,19</sup> and of the fluorescence recovery following a pulsed MW field<sup>15</sup> provide data on the transition frequencies between triplet spin substates, the intersystem crossings rates for different triplet substates, isotopic effects,<sup>16,19,20,22</sup> etc., for single pentacene (Pc) molecules in *p*-terphenyl (PT) crystals (the "hydrogen atom" of SMS). Furthermore, owing to the long-time scale character of FDMR experiments where temporal averaging replaces conventional ensemble averaging,<sup>14</sup> coherent transient phenomena such as nutation<sup>14</sup> and the two-pulse Hahn spin echo<sup>17</sup> have been observed on single triplet spins and used to characterize the dynamical processes in the embedding matrix that contribute to triplet spin dephasing.

In the simplest case the information about triplet spin dephasing is reduced to the determination of a dephasing time  $T_2$  obtained by fitting the FDMR experimental data using calculations based on the well-known Bloch equations (BE's). Such descriptions<sup>15</sup> have provided approximate agreement with observations but could not explain some important features of the experimental data, especially in the case of strong MW fields. Meanwhile, as was recognized long ago,<sup>23-25</sup> the BE-based theories are correct only when the dynamics of the embedding matrix (bath) is very fast so that one can neglect the correlation time  $\tau_c$  of the triplet-spin-matrix interactions in comparison with the other rel-

evant characteristic times (e.g., with  $T_2$ ). At liquid helium temperatures the main source for pure dephasing of a triplet spin of a typical chromophore guest molecule in an organic host matrix originates from the fluctuations  $U^I$  of its resonance frequency due to interactions with nuclear (proton) spins in the host matrix<sup>26</sup> which perform mutual flip-flops in a random way and modulate stochastically the triplet substate energies via hyperfine dipole-dipole interactions. From the analysis<sup>26</sup> of phosphorescence-detected magnetic resonance (PDMR) experiments on ensembles of triplet spins, one can expect the fluctuations  $U^I$  to be slow in the sense of the Kubo classification:<sup>27</sup>  $\sigma \gg \nu$ , where  $\sigma$  is the variance of the fluctuations  $U^I$  and  $\nu$  is the average proton flip-flop rates. Under these conditions there is no longer a time scale separation between the correlation time  $\tau_c \sim \nu^{-1}$  of the bath and the dephasing time  $T_{deph}$  of a triplet spin. As a consequence, the standard Markov-type BE's are no longer valid and new, non-Markovian effects begin to be important (see, e.g., Refs. 28–35 and references therein). The relaxation of a triplet spin then depends not only on the state which it is in, but also on its past history—the pathway through which it reached that state. In other words, memory effects begin to play a role. In particular, one of the most important expected non-Markovian effects is the dependence of fluctuation-induced triplet spin dephasing on the strength of an applied MW field. A sufficiently strong MW field can suppress completely the dephasing.<sup>23</sup> This effect is analogous to “spin locking” known long ago in the PDMR spectroscopy of an ensemble of spins (see, e.g., Refs. 36–39). In the present paper, we use the stochastic approach of Kubo to describe the pure dephasing of a triplet spin due to the host nuclear spin dynamics and study its manifestations in different FDMR phenomena in guest-host systems with slow dephasing fluctuations  $U^I$ . To be more specific we use in our analysis the parameter values typical for the Pc+PT system. We demonstrated the agreement between theory and experiments on the observations of power-broadened FDMR line shapes of single Pc molecules in PT crystals which show a pronounced effect of MW-field-suppressed dephasing. Moreover, we discuss the time-domain FDMR phenomena on single molecules: the FDMR free induction decay and the FDMR Hahn echo. Preliminary versions of the theory and of its applications to describe previous experimental data on (i) the power-broadened FDMR line shapes, (ii) the transient nutations, (iii) the fluorescence intensity correlation function, and (iv) the FDMR Hahn echo on single triplet-state Pc molecules in PT crystal have appeared in Refs. 40–42.

The organization of the paper is as follows. In Sec. II we introduce the model of a five-level single molecule driven by optical and MW fields. Starting from a stochastic Liouville equation for the molecule with fluctuating triplet spin transition frequency, we deduce the equations for the density matrix of a molecule averaged over the fluctuations  $U^I$ . An additional averaging over an inhomogeneous distribution of possible frequencies of resonant triplet spin transition frequencies, resulting from different proton spin configurations of the Pc molecule, is also discussed. A model of  $N$  random telegraph processes for the fluctuations  $U^I$  is introduced and an exact set of equations is derived which can be used to calculate the average density matrix of a molecule. In the case when the intersystem crossing rates  $k_j^i$  are small in com-

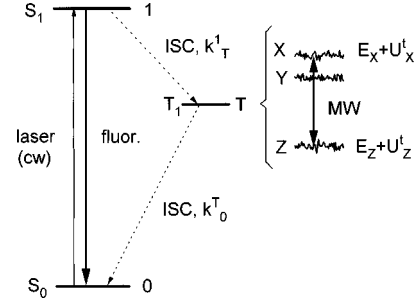


FIG. 1. Model of a five-level system for a single chromophore molecule in a low-temperature matrix.  $S_0$  is the lowest singlet state,  $S_1$  is the first excited singlet state, and  $T = X, Y, Z$  are three substates of the first excited zero-field-split triplet state  $T_1$ . Intersystem crossings (ISC's)  $S_1 \rightarrow T$  and  $T \rightarrow S_0$  occur with rates  $k_T^1$  and  $k_0^T$ , respectively. The laser field is in resonance with the  $S_1$ - $S_0$  transition while microwaves are resonant with the  $X$ - $Z$  transition. Triplet substate energies  $E_T$  fluctuate due to stochastic interactions  $U_T^I$  of the triplet electron spin with the host matrix nuclear (proton) spins undergoing mutual flip-flops in a random way.

parison with the host spin flip-flop rate  $\nu$ , these equations reduce to much simpler equations describing the isolated evolution of two resonant triplet spin sublevels only. In Sec. III we apply the general theory to study frequency- and time-domain FDMR phenomena including (i) the power-broadened FDMR line shape (Sec. III A) and (ii) the FDMR free induction (FI) decay and the FDMR Hahn echo (Sec. III B). Simple analytical expressions for the FDMR signals are obtained when  $k_j^i \ll \nu$ . Experimental data on power-broadened FDMR  $X$ - $Z$  transition line shapes of single Pc molecules in PT crystals are fit at low, medium, and high MW field strengths with  $\nu/2\pi = 30$  kHz and  $\sigma/2\pi = 85$  kHz. It is shown that the FDMR FI decay rate after a  $\pi/2$  pulse in the Pc+PT system is determined mainly by the inhomogeneous distribution while the FDMR Hahn echo decay can serve as a sensitive tool to derive information about the model parameters  $\nu$  and  $\sigma$ . Section IV concludes the article with a brief discussion of the main results. The Appendix contains some lengthy calculations needed to derive the basic equations (16a)–(16d). Additionally, we construct and discuss in the Appendix the other completely equivalent version of these equations, being well known as the equations of the sudden modulation theory.

## II. THEORY

### A. Model and general discussion

We describe a single guest chromophore molecule as a five-level quantum system (Fig. 1) where  $|0\rangle$  is the ground singlet state  $S_0$  of the molecule,  $|1\rangle$  is its excited singlet state  $S_1$ , and  $|T\rangle$  ( $T = X, Y, Z$ ) are three substates into which the lowest excited triplet state  $T_1$  is split (in zero magnetic field) by magnetic dipolar interaction of the two unpaired triplet electrons.<sup>43</sup> All molecular states are zero-phonon states because they are the only essential ones due to a very fast internal conversion processes within their respective vibrational-state manifolds.

The molecule is driven by a saturating cw laser field  $E(t) = E^+ \exp(-i\omega_0 t) + \text{c.c.}$  that is in near resonance with the optical molecular transition 1-0. In general, the optical fre-

quency  $\omega_{10}$  of a single guest molecule in a low-temperature host matrix is subjected to spectral diffusion which can arise, for example, as a result of the interaction of the molecule with neighboring two-level systems in the host matrix which undergo phonon-assisted tunneling transitions that lead to instantaneous jumps in the molecule's optical transition frequency. There have been numerous experimental (see, e.g., Refs. 5 and 44–47) and theoretical<sup>48,49</sup> studies of such jumplike optical spectral diffusion of a single molecule in crystal or amorphous matrices. However, spectral diffusion does not play a role in the FDMR experiments,<sup>14,15,17</sup> which are of main interest in this article, since the samples of Pc+PT mixed crystals are specially prepared to suppress spectral diffusion (the samples have no domain structure responsible for presence of structural tunneling two-level systems and thus for spectral diffusion<sup>48</sup>). Let us recall also that previous ensemble experiments on Pc+PT mixed crystals<sup>50</sup> have also revealed the complete linewidth of the Pc optical transition to be lifetime limited; i.e., it had no additional pure dephasing contribution resulting from any frequency fluctuations. Therefore, below we treat the optical transition 1-0 as having constant frequency. Absorption of a photon from the optical field brings the molecule from ground state 0 to excited state 1 with an induced absorption rate  $B_{10}u_{opt}$  ( $B_{10}$  is the differential Einstein coefficient and  $u_{opt}$  is the optical radiation density) while the spontaneous emission events having rate  $A$  return it back to state 0 with emission of fluorescence photons. Counts of these fluorescence photons by an appropriate detector provide a measured signal in the FDMR technique.

By means of intersystem crossings (ISC's) the singlet states  $S_0, S_1$  of a molecule are connected with the triplet substates  $T$ . Owing to ISC events  $S_1 \rightarrow T$  the molecule relaxes from state 1 to the triplet substates  $T$  with rates  $k_T^1$ . The ISC processes result also in transitions from substates  $T$  to the ground singlet state 0 with rates  $k_0^T$ . As a rule, the population/depopulation rates  $k_T^1, k_0^T$  of triplet substates are different for different substates  $T$ , depending on the symmetry of the molecule. In particular, most of the planar aromatic molecules which are of main interest in this article have rates  $k_T^1$  and  $k_0^T$  of the two inplane sublevels  $X, Y$  which are similar and higher by a factor of  $\sim 10$ – $100$  than those of the out-of-plane sublevel  $Z$ .<sup>51</sup> As a result, the average steady-state populations of the triplet sublevels of the molecule excited by a resonant cw optical field and subjected to ISC transitions are inherently different and it is this circumstance that provides a physical basis for the FDMR technique. For Pc molecules in PT crystal the rates  $k_T^1$  and  $k_0^T$  have been determined in Ref. 15 to be equal to  $k_X^1 = 66 \times 10^3 \text{ s}^{-1}$ ,  $k_Y^1 = 29 \times 10^3 \text{ s}^{-1}$ ,  $k_Z^1 = 0.28 \times 10^3 \text{ s}^{-1}$ , and  $k_0^X = 20 \times 10^3 \text{ s}^{-1}$ ,  $k_0^Y = 20 \times 10^3 \text{ s}^{-1}$ , and  $k_0^Z = 1.2 \times 10^3 \text{ s}^{-1}$  (it should be noted that the investigations of Ref. 18 have revealed variations of these rates among different single Pc molecules, but to simplify matters, we use the above values in our calculations). Given these rates and a spontaneous emission rate  $A = 43 \times 10^6 \text{ s}^{-1}$  for the Pc singlet-singlet transition,<sup>15</sup> one finds that, under conditions of optical saturation (for an optical Rabi frequency  $2V = 92 \times 10^6 \text{ s}^{-1}$  where  $V = -p_{10}E^+/\hbar$  and  $p_{10}$  is the transition 1-0 dipole moment matrix element) the average population of the substate  $X$  in steady state will be the largest among

the five levels:  $\rho_{XX}^{(0)st} \approx 0.4582$ ,  $\rho_{YY}^{(0)st} \approx 0.2013$ ,  $\rho_{ZZ}^{(0)st} \approx 0.0324$ ,  $\rho_{11}^{(0)st} \approx 0.1388$ , and  $\rho_{00}^{(0)st} \approx 0.1623$ .

In FDMR spectroscopy, two of the three molecular triplet substates are coupled by a cw or pulsed MW field  $B(t) = B^+ \exp(-i\omega t) + \text{c.c.}$ , resulting in a rearrangement of triplet substates populations which, in turn, modifies the fluorescence intensity in the singlet-singlet channel. Moreover, the MW field creates a coherent superposition of the triplet substates. To be more specific we will assume in what follows that the MW field is nearly resonant with the transition  $X$ - $Z$  ( $\omega \approx \omega_{XZ}$ ). In contrast to the optical channel 1-0, the frequency  $\omega_{XZ}$  is subjected to fluctuations; i.e., it is a stochastic process:  $\omega_{XZ}^t = \bar{\omega}_{XZ} + U^t$  ( $U^t = U_X^t - U_Z^t$ ,  $\langle U^t \rangle = 0$ ). In organic impurity crystals at low temperature the fluctuations  $U^t$  originate mainly from the interactions of a triplet electron spin with fluctuating nuclear (proton) spins in the host matrix.<sup>26</sup> As is well known, the fluctuations destroy the MW-field-induced coherence or, in other words, result in a pure dephasing of the transition  $X$ - $Z$ . The characteristics of fluctuations  $U^t$  (correlation time  $\tau_c$ , variance  $\sigma$ , etc.) and, as well, their manifestations in various FDMR phenomena are of the main interest in this article. Again, it should be understood that due to irregularities of the host crystal lattice, the statistical characteristics of fluctuations  $U^t$  can vary from molecule to molecule and the great advantage of single-molecule spectroscopy is the opportunity to study the distribution of these characteristics among different single chromophore molecules.

In the presence of optical and MW fields and of ISC transitions, the single molecule acts as a five-state system exhibiting quantum jumps of three types: (i) jumps between singlet states  $S_0$  and  $S_1$  accompanied by absorption or emission of photons, (ii) jumps between singlet and triplet states (transitions  $S_1 \rightarrow T$  and  $T \rightarrow S_0$ ) which result in emission of phonons, and (iii) jumps between resonant triplet substates  $X$  and  $Z$  with induced absorption or emission of MW field quanta. Typically the spontaneous emission rate  $A$  is much larger than the ISC transition probabilities  $k_T^1$ ,  $k_0^T$  ( $A \sim 10^8 \text{ s}^{-1}$ ,  $k_T^1, k_0^T \sim 10^2$ – $10^4 \text{ s}^{-1}$ ). In a saturating optical field, there are many fluorescence photons emitted before the molecule is shelved in one of the long-lived triplet substates. After the molecule returns back to the ground state due to the ISC  $T \rightarrow 0$  transition, the absorption-emission cycles in the 1-0 optical channel are restored until the next ISC transition to the triplet state. As a result, fluorescence photons emitted by a molecule are grouped in bunches of average duration of the order of  $2/k_T^1$  (Ref. 7) separated by totally dark intervals whose average duration is determined by the average residence time of a molecule in the triplet state. Thus, the detailed stochastic dynamics of a single molecule is rather complicated and is characterized by many time scales. In principle, this jumplike evolution of a molecule can be described (and simulated) in terms of continuous quantum measurement theory,<sup>52</sup> in which emission of fluorescence photons on the 1-0 transition and emission of phonons on ISC transitions  $1 \rightarrow T$ ,  $T \rightarrow 0$ , constitute measurements that result in the projection of a molecule into a particular quantum state. Continuous measurement theory has been applied previously to a simple model system, consisting of a single, laser-driven, two-level chromophore molecule strongly

coupled to a single tunneling two-level system (TLS) in an amorphous host matrix.<sup>53</sup> In this case, the molecular quantum-jump dynamics is described in terms of a stochastic (four-state) semi-Markov process. The quantum Liouville equations for the density operator of the combined quantum system “molecule+TLS” were constructed within the context of continuous measurement theory and used to calculate the conditional jump probabilities and the waiting time distributions. An extension of the theory of Ref. 53 to our five-level molecule can be performed in a straightforward way.

In many cases, however, the above detailed description of a single molecule’s evolution is excessive and, from a theoretical viewpoint, one can simplify matters by obtaining only some average information on the state of the molecule. In the case of FDMR spectroscopy of single triplet spins, one monitors the average fluorescence intensity  $\langle I^t \rangle$  or the second-order correlation function of the fluorescence intensity  $g^{(2)}(\tau) = \langle I^t I^{t+\tau} \rangle / \langle I^t \rangle^2$  as a function of the applied MW field. Owing to the inherently low signal/noise ratio, it is necessary to accumulate signals during a rather long period of time. Usually the duration of a full FDMR experiment is very large in comparison with the average total length of “bright” and “dark” periods of fluorescence. For example, the observations of FDMR line shapes, which show up as changes in the average fluorescence intensity when one scans slowly the cw MW field frequency through the EPR resonance  $\omega_{XZ}$  (or  $\omega_{YZ}$ ), consists of many scans with the typical time for each scan equal to 10 s (Ref. 15) and the full experiment taking a few minutes. In experiments on FDMR coherent transients such as Ref. 14 on FDMR nutation or Ref. 17 on a FDMR echo, a molecule is subjected to a sequence of MW pulses, each representing a “single transient experiment.” The sequence of pulses is repeated many times with the delay between the sequences sufficiently long to allow the molecule to return to its steady-state response in the absence of MW fields. The fluorescence photons are counted during some observation time  $t_{obs}$  after the last pulse in a single sequence which, typically, is equal to 1 ms. Thus, during a complete FDMR experiment using either cw or pulsed MW fields, a molecule has time to enter the triplet state many times, interacting there each time with the MW field and experiencing a random change  $\Delta\varphi = \int dx U^x$  in the relative phase of the resonant substates  $X$  and  $Z$  in accordance with the specific history of stochastic frequency fluctuations  $U^t$  during the triplet state lifetime. Long-time-scale FDMR experiments average over individual histories of a molecule in a triplet state and, as a result, the theoretical description of such experiments can be given in terms of the density matrix of the system. Conventionally, this method is associated with some ensemble averaging which, in ordinary spectroscopy, is just the average over many different molecules. In the case of a single triplet electron spin this ensemble averaging is replaced by time averaging<sup>14</sup> over ensembles of experiments on a single molecule. Both kinds of averaging are equivalent, in accordance with the ergodic principle. Thus the FDMR observables [the average fluorescence intensity  $\langle I^t \rangle$  and the second-order correlation function of the fluorescence intensity  $g^{(2)}(\tau)$ ] are proportional to the excited singlet-state population  $\langle \rho_{11}^t \rangle$  averaged over fluctuations  $U^t$  and it will be our aim below to calculate this quantity.

An additional feature of FDMR experiments is the necessity to take into account the distribution  $P(\bar{\omega}_{XZ})$  of possible frequencies  $\bar{\omega}_{XZ}$  of the transition  $X$ - $Z$  with frequencies  $\bar{\omega}_{XZ}$  corresponding to some specific configuration of proton spins of a molecule. This configuration introduces a shift in the energies of substates  $X, Z$  owing to hyperfine interactions (hfi’s) between a triplet electron spin  $S = 1$  and the surrounding proton spins.<sup>12,15</sup> During the triplet-state lifetime the triplet electron spin influences strongly the proton spins at the chromophore molecule; consequently they become energetically detuned from the proton spins in the host matrix and, for that reason, cannot participate in energy-conserving mutual flip-flops with the bulk proton spins. That is why these chromophore molecule proton spins are usually termed as “frozen” spins or a “frozen configuration” of spins. After the molecule returns back to the ground singlet state the electron spin vanishes, its influence on the chromophore molecule proton spins disappears, and they acquire an opportunity to change their spin state through flip-flops with proton spins in the host matrix. Therefore, when a molecule reenters the triplet state, the configuration of its proton spins can differ from the previous one and, as a consequence, the frequency  $\bar{\omega}_{XZ}$  of the transition  $X$ - $Z$  can be changed slightly. During the long FDMR experiment time all possible proton spin configurations are sampled and thus the population  $\langle \rho_{11}^t \rangle$  of state 1 must additionally be averaged over the distribution  $P(\bar{\omega}_{XZ})$ :  $\bar{\rho}_{11}^t = \int d\bar{\omega}_{XZ} \langle \rho_{11}^t \rangle P(\bar{\omega}_{XZ})$ . It is this doubly averaged population  $\bar{\rho}_{11}^t$  of the excited singlet state which is monitored in FDMR experiments. In fact, the distribution  $P(\bar{\omega}_{XZ})$  is the single-molecule equivalent of a conventional inhomogeneous frequency distribution. In the case of the Pc molecule the distribution  $P(\bar{\omega}_{XZ})$  is strongly asymmetric with full width at half maximum (FWHM)  $\sim 5$  MHz.<sup>15,54</sup> Note that, in principle, one can modify the distribution  $P(\bar{\omega}_{XZ})$  by deuteration (by using the other chemical substitutions) of chromophore molecules or of guest crystal molecules as well. For example, in the case of Pc+PT samples with deuterated Pc/PT molecules<sup>19–22</sup> the distribution  $P(\bar{\omega}_{XZ})$  is practically eliminated due to strongly ( $\sim 40$  times) decreased hfi’s resulting from a reduced deuterium nuclear moment which is approximately 6 times smaller than that of a proton. Below we will discuss the FDMR experiments made using usual nondeuterated samples with nonisotopically substituted carbons.

First we discuss the calculation of  $\langle \rho_{11}^t \rangle$ . The standard method of solution is to construct equations for the averaged density matrix  $\langle \rho_{ij}^t \rangle$ , which are usually referred to as master equations (ME’s), and then to solve them with respect to the desired element  $\langle \rho_{11}^t \rangle$ . The simplest form of the master equations is the well-known BE’s.<sup>24,55</sup> These equations incorporate the ISC transitions and the spontaneous transition  $1 \rightarrow 0$  through rate coefficients in equations for diagonal density matrix elements  $\langle \rho_{ii}^t \rangle$ . The transitions contribute also to the dephasing rates of relevant transitions. An additional source for dephasing is fluctuations of the transition frequency, usually referred to as pure dephasing. In the BE’s such effects are incorporated by additive contributions to the dephasing rate coefficients. For example, the decay rate of the coherence between the triplet substates  $X$  and  $Z$  is equal



is the matrix accounting for the ISC processes with  $k_T = k_X^1 + k_Y^1 + k_Z^1$ ,  $k_0^{X\pm Z} = (k_0^X \pm k_0^Z)/2$ , and  $k_{X-Z}^1 = (k_X^1 - k_Z^1)/2$ . The second term in Eq. (1) takes into account the effects of frequency fluctuations  $U^t$  on the coherences  $\rho_{XZ}^t, \rho_{ZX}^t$ ; therefore, the matrix  $F$  has two nonzero elements only:

$$F = \begin{pmatrix} Z_{5,5} & Z_{3,5} & & & \\ & 1 & 0 & 0 & \\ Z_{5,3} & 0 & 0 & 0 & \\ & 0 & 0 & -1 & \end{pmatrix}. \quad (6)$$

The vector  $r_0$  in Eq. (1) has components  $r_{0i} = (0, 0, k_0^{X+Z}, 0, 0, 0, -k_0^{X-Z}/2, 0)$ . This inhomogeneous term results from our having used the normalization condition  $\rho_{XX}^t + \rho_{ZZ}^t = 1 - (\rho_{11}^t + \rho_{00}^t + \rho_{YY}^t)$  to eliminate  $\rho_{XX}^t + \rho_{ZZ}^t$ . Note that Eq. (1) without the second term coincides with the BE's written in matrix form for the five-level system, if one puts in the latter  $T_{2XZ}^{-1} = k_0^{X+Z}$ , i.e., supposes pure dephasing of the  $X$ - $Z$  transition to be absent. Furthermore, if the MW field is absent, one can put, in Eq. (1),  $D = D_V + D_K$  and cancel the second term since the coherences  $\rho_{XZ}^t, \rho_{ZX}^t$  vanish and the fluctuations  $U^t$  are unimportant in this limit.

Our choice for the vector  $r^t$ , which is composed of density matrix elements in a different way than is usually adopted in the conventional ‘‘Feynman-Vernon-Helwarth’’ vector description of two-level system dynamics,<sup>55,62</sup> provides an opportunity to express the matrices  $D_W$  and  $F$  in terms of the standard spin matrices  $S_x$  and  $S_z$  ( $S = 1$ ) in a Cartesian representation<sup>63</sup>

$$D_W = \begin{pmatrix} Z_{5,5} & Z_{3,5} \\ Z_{5,3} & -i(\delta S_z + 2WS_x) \end{pmatrix}, \quad F = \begin{pmatrix} Z_{5,5} & Z_{3,5} \\ Z_{5,3} & S_z \end{pmatrix}. \quad (7)$$

Then, using the commutation rules for these matrices  $[S_z, S_x] = iS_y$ ,  $[S_y, S_z] = iS_x$ ,  $[S_x, S_y] = iS_z$ , we are able to perform some calculations analytically (see below).

For times  $t \ll (k_j^i)^{-1}$ , when one can neglect the ISC transitions, it is possible to omit the matrix  $D_K$  in Eq. (2) and then, taking into account the commutativity of the matrix  $D_V$  with the matrices  $D_W$  and  $F$ , obtain from Eq. (1) the reduced closed matrix equation

$$\dot{\tilde{r}}^t = -i(\delta S_z + 2WS_x)\tilde{r}^t - iS_z U^t \tilde{r}^t \quad (8)$$

for the three-dimensional vector  $\tilde{r}^t$  having components  $\tilde{r}_\alpha^t = (\rho_{XZ}^t, \Delta^t, \rho_{ZX}^t)$  ( $\alpha = 1, 2, 3$ ) describing the evolution of the triplet substates  $X$  and  $Z$  under the action of the MW field. The two-level system described by Eq. (8) can be considered as ‘‘closed’’ on this time scale with total population  $\rho_{XX}^t + \rho_{ZZ}^t$  constant, but not equal to unity. Note that the description of a molecule as a two-level system, consisting of resonant triplet substates, is conventionally used in theories of optically detected magnetic resonance spectroscopy (see, e.g., Ref. 37) and is especially effective when one considers transient FDMR phenomena (see Sec. III B).

Returning to Eq. (1), averaging over realizations of the stochastic process  $U^t$ , and substituting the formal solution of Eq. (1) into  $-iF\langle U^t r^t \rangle$  one obtains the evolution equation for the average vector  $R^t = \langle r^t \rangle$ :

$$\dot{R}^t = DR^t - \int_0^t d\tau L^{t-\tau} \langle U^t U^\tau r^\tau \rangle + r_0, \quad L^{t-\tau} = F e^{D(t-\tau)} F. \quad (9)$$

This equation, however, is not a ME owing to the presence of the correlation function  $\langle U^t U^\tau r^\tau \rangle$  in the integral term. The simplest case, when Eq. (9) becomes closed with respect to the vector  $R^t$ , is that of  $\delta$ -correlated fluctuations  $U^t$ , when  $\langle U^t U^\tau r^\tau \rangle = 2K_{XZ} \delta(t-\tau) R^t$ . In that limit, the integral over time in Eq. (9) disappears, reducing it to the standard Bloch-type master equation for a five-level quantum system having the  $X$ - $Z$  transition pure dephasing rate equal to  $K_{XZ}$ . In real systems, where the correlation time is nonvanishing, the correlation function  $\langle U^t U^\tau r^\tau \rangle$  is nonzero for  $|t-\tau| \leq \tau_c$ , thus requiring one to take into account non-Markovian effects, i.e., the ‘‘memory’’ of the history of the system on a time scale  $\sim \tau_c$ . One such effect is the dependence of dephasing processes on the MW field characteristics owing to the presence of matrix  $D_W$  in the kernel  $L^{t-\tau} = F e^{D(t-\tau)} F$  of the integral term in Eq. (9). It follows from Eq. (6) that the matrix kernel  $L^{t-\tau}$  has only four nonzero elements  $L_{66}^t = (\exp Dt)_{66}$ ,  $L_{68}^t = -(\exp Dt)_{68}$ ,  $L_{86}^t = -(\exp Dt)_{86}$ , and  $L_{88}^t = (\exp Dt)_{88}$ ; i.e., the integral terms in Eqs. (9) appear only in the equations for the components  $R_6^t = \langle \rho_{XZ}^t \rangle$ ,  $R_8^t = \langle \rho_{ZX}^t \rangle$  along with the correlation functions  $\langle U^t U^\tau \rho_{XZ}^t \rangle$ ,  $\langle U^t U^\tau \rho_{ZX}^t \rangle$ .

If the fluctuations are fast on a time scale  $\sim (k_j^i)^{-1}$ , one can average the reduced stochastic equation (8) over fluctuation histories  $U^t$  to obtain the equation for  $\tilde{R}^t = \langle \tilde{r}^t \rangle$ :

$$\dot{\tilde{R}}^t = -i(\delta S_z + 2WS_x)\tilde{R}^t - \int_0^t d\tau S_z e^{-i(\delta S_z + 2WS_x)(t-\tau)} S_z \langle U^t U^\tau \tilde{r}^\tau \rangle, \quad (10)$$

whose correlation function  $\langle U^t U^\tau \tilde{r}^\tau \rangle$  is nonvanishing for  $|t-\tau| \leq \tau_c$  only. The kernel  $\tilde{L}^{t-\tau} = S_z e^{-i(\delta S_z + 2WS_x)(t-\tau)} S_z$  of this equation contains only four nonzero elements and can be calculated explicitly using commutation properties of spin  $S = 1$  operators. Thus, one can use the well-known relations  $\exp\{-i(\delta S_z + 2WS_x)t\} = \exp\{-i\Omega(cS_z + sS_x)t\} = \exp\{-i\Omega S_z' t\}$ ,  $\exp\{-i(\delta S_z + 2WS_x)t\} = \exp\{-i\Omega(cS_z + sS_x)t\} = \exp\{-i\Omega S_z' t\} = \exp\{-i\theta S_y\} \exp\{-i\Omega S_z t\} \exp\{i\theta S_y\}$ , where  $c = \cos \theta = \delta/\Omega$ ,  $s = \sin \theta = 2W/\Omega$ ,  $\Omega = (\delta^2 + 4W^2)^{1/2}$  is the generalized Rabi frequency of the MW field, and  $S_z' = cS_z + sS_x = \exp\{-i\theta S_y\} S_z \exp\{i\theta S_y\}$  is the  $S_z$  operator in the ‘‘MW-field-dressed-state’’ basis (the transformation to this basis is performed by the unitary transformation  $E' = \exp\{-i\theta S_y\} E \exp\{i\theta S_y\}$ ), and operator identities  $\exp\{\beta S_i\} = I - S_i^2 + S_i^2 \text{ch} \beta + S_i \text{sh} \beta$  ( $i = x, y, z$ ),<sup>63</sup> to obtain the operator relation  $\exp\{-i\Omega(cS_z + sS_x)t\} = I - iS_z' \sin \Omega t + S_z'^2 (\cos \Omega t - 1)$ . Using these relations, one finds

$$\tilde{L}^{t-\tau} = \begin{pmatrix} f_1^{t-\tau} & 0 & f_2^{t-\tau} \\ 0 & 0 & 0 \\ f_2^{t-\tau} & 0 & (f_1^{t-\tau})^* \end{pmatrix}, \quad (11)$$

where

$$f_1^t = \frac{s^2}{2} + \left( c^2 + \frac{s^2}{2} \right) \cos \Omega t - ic \sin \Omega t, \quad (12a)$$

$$f_2^t = -\frac{s^2}{2}(\cos \Omega t - 1). \quad (12b)$$

In turn, the kernel  $L^{t-\tau}$  of the complete equation (9) can be expressed, at small times  $t \ll (k_j^i)^{-1}$ , in terms of the kernel  $\tilde{L}^{t-\tau}$  of the reduced equation (11) as follows:

$$L^{t-\tau} = \begin{pmatrix} Z_{5,5} & Z_{3,5} \\ Z_{5,3} & \tilde{L}^{t-\tau} \end{pmatrix}. \quad (13)$$

For the systems under discussion, typical correlation times  $\tau_c$  are of the order of the inverse average frequency of proton spin flip-flops in the host matrix (approximately several  $\mu$ s), while typical triplet substate lifetimes due to ISC processes are on the order of tens of microseconds or more. Since the kernel in Eq. (9) is nonvanishing only for times of order of the correlation time  $\tau_c$ , which defines the ‘‘lifetime’’ of the correlation function  $\langle U^t U^\tau r^\tau \rangle$ , one can use the approximate form of the kernel (11)–(13) in Eq. (9). Furthermore, if  $\Omega \tau_c \gg 1$ , then  $\sin \Omega(t-\tau)$  and  $\cos \Omega(t-\tau)$  oscillate rapidly on a time scale of  $\tau_c$ , allowing one to neglect the contributions from oscillating terms in Eqs. (12a) and (12b). As a result, the kernel in Eq. (9) can be approximated as

$$L^{t-\tau} = \frac{s^2}{2} \begin{pmatrix} Z_{5,5} & & Z_{3,5} & \\ & 1 & 0 & 1 \\ Z_{5,3} & 0 & 0 & 0 \\ & & 1 & 0 & 1 \end{pmatrix}. \quad (14)$$

The dephasing terms in this case are expressed in Eq. (9) through the time integrals of the correlation functions  $\langle U^t U^\tau \rho_{XZ}^\tau \rangle$ ,  $\langle U^t U^\tau \rho_{ZX}^\tau \rangle$ .

In some cases the correlation function  $\langle U^t U^\tau r^\tau \rangle$  can be factored as  $\langle U^t U^\tau \rangle R^\tau$ , converting Eq. (9) into a ME. For example, in the case of weak and fast fluctuations  $U^t$ , when  $\sigma \tau_c \ll 1$ ,  $\langle U^t U^\tau r^\tau \rangle \approx \langle U^t U^\tau \rangle R^\tau$  [this approximation is consistent with a perturbative solution of Eq. (9) to second order in  $U^t$  (Ref. 64)]. In the case of strong and slow fluctuations  $\sigma \tau_c \gg 1$ , which is of the main interest in this paper, the calculation of the correlation function  $\langle U^t U^\tau r^\tau \rangle$  is possible only using some specific stochastic models for the fluctuations  $U^t$  whose statistical properties provide some kind of relation between  $\langle U^t U^\tau r^\tau \rangle$  and  $R^\tau$ . In particular, within the model of a symmetric random telegraph (RT) process for the fluctuations  $U^t$ , where the quantity  $U$  undergoes instantaneous jumps between two values  $U = \sigma$  and  $U = -\sigma$  with equal transition probability densities  $\varphi_{\sigma \rightarrow -\sigma} = \varphi_{-\sigma \rightarrow \sigma} = \nu$  [the correlation function for the RT process is  $\langle U^t U^0 \rangle = \sigma^2 \exp(-2\nu t)$ , correlation time  $\tau_c = (2\nu)^{-1}$ ], the decoupling procedure  $\langle U^t U^\tau r^\tau \rangle = \langle U^t U^\tau \rangle R^\tau$  is exact<sup>64,65</sup> and valid for arbitrary ratios of the parameters  $\sigma, \nu$ . For this reason the RT model is widely used in stochastic theories of dephasing processes, especially, in the theory of the field-modified pure dephasing (see, e.g., Refs. 29–31, 66, and 67).

The RT model, however, is a highly simplified stochastic model. It provides a proper description of experimental data for systems with weak fluctuations only for which the ‘‘narrowing’’ parameter  $\sigma^2 \tau_c^2 \ll 1$ . Physically this model corresponds to the situation where there is only one nuclear (proton) spin  $S = 1/2$  in the vicinity of a chromophore molecule

and it is this neighboring spin, undergoing transitions between its states at random moments of time, which modulates stochastically the triplet substate energies through the diagonal part of its dipole-dipole interaction with the triplet electron spin. In real molecular systems there are many flipping proton spins around an impurity molecule and, therefore, in this case it seems to be more suitable to model the fluctuations  $U^t$  by a sum of  $N$  independent random telegraph processes,  $U^t = \sum_{k=1}^N U_k^t$ , with each component process  $U_k^t$  having the same jump frequency  $\nu$ , equal to the average flipping rate of proton spins in the host matrix, but different (in general case) variances  $\sigma_k$  according to different distances between the proton spins and the triplet electron spin. Below we refer to this model as an  $N$  RT. As is known well, in the case of equal variances  $\sigma_k$  at  $N \rightarrow \infty$  the  $N$  RT process becomes, according to the central limit theorem, a Gaussian-Markovian (normal) process. For this reason it is often named a ‘‘pre-Gaussian process.’’<sup>68</sup> Note, however, that with different variances  $\sigma_k$  this Gaussian limit is not valid (see, e.g., Ref. 69).

The  $N$  RT model has been used previously in various theories to describe dephasing processes due to spin-spin interactions and to calculate decays of coherent transients (spin echoes, free induction decay, etc.) in spin systems with slow frequency fluctuations.<sup>70–72</sup> Most recently<sup>48,49</sup> this model has been applied in SMS spectroscopy to describe the observations<sup>5</sup> of spectral diffusion in an optical singlet-singlet transition of single Pc molecules in PT crystals due to the interactions of a Pc molecule with a multitude of tunneling TLS’s formed by the two lowest states in a double-well potential describing librations of the central phenyl ring of terphenyl molecules between two possible stable positions.<sup>48</sup> It should be emphasized that here we extend the previous  $N$  RT model stochastic theories in that our calculations of the response of a molecule to external fields are based on *exact* equations [Eqs. (16a)–(16d)] describing the experimentally monitored average behavior of a molecule. In contrast to previous theories, these equations take into account *simultaneous* effects on a molecule both of stochastic fluctuations  $U^t = \sum_{k=1}^N U_k^t$  and of external fields and, in principle, they are applicable to calculate *any* desired response of a molecule to external fields (not only of the echo and FI decay signals as in Refs. 70 and 71 or of the linear line shape as in Ref. 48). In particular, these equations take into account the influence of the MW field on the triplet electron spin dephasing induced by flipping proton spins and thus make it possible to describe in a proper way the suppression of dephasing by MW fields. Note that the assumption of equal up and down jump rates for the component processes  $U_k^t$  (the high-temperature assumption) is used here for simplicity and can be eliminated straightforwardly within the context of the model [see Eq. (A4) in the Appendix].

Each component RT process  $U_k^t$  is characterized by a correlation function of the form  $\langle U_k^t U_k^\tau \rangle_{(k)} = \sigma_k^2 \exp\{-2\nu(t-\tau)\}$ , where  $\langle \dots \rangle_{(k)}$  denotes averaging over all realizations of the process  $U_k^t$ . Using the known properties of RT process,  $(U_k^t)^2 = \sigma_k^2$  and  $\langle U_k^t U_k^\tau r^\tau \rangle_{(k)} = \langle U_k^t U_k^\tau \rangle_{(k)} \langle r^\tau \rangle_{(k)}$ , and keeping in mind that the vector  $r^t$  is a functional of all processes  $U_k^t$ , one can represent the correlation function  $\langle U^t U^\tau r^\tau \rangle$  in Eqs. (9) as

$$\langle U^t U^\tau r^\tau \rangle = e^{-2\nu(t-\tau)} \left( \sum_{k=1}^N \sigma_k^2 R^\tau + 2 \sum_{k,l(k \neq l)}^N \langle U_k^\tau U_l^\tau r^\tau \rangle \right), \quad (15)$$

i.e., express the correlation function in terms of the *one-time* averages  $R^\tau$  and  $\langle U_k^\tau U_l^\tau r^\tau \rangle$ . The angular brackets  $\langle \dots \rangle$  without indices here mean the total average over possible realizations of *all* component processes  $U_k^\tau$ . Clearly, within the  $N$  RT model the decoupling procedure  $\langle U^t U^\tau r^\tau \rangle \approx \langle U^t U^\tau \rangle R^\tau$  is equivalent to neglecting the second sum in Eq. (15) which is valid only if the fluctuations  $U^t$  are fast and weak so that the condition  $\sigma \leq 2\nu$  is fulfilled, where  $\sigma = \sqrt{\sum \sigma_k^2}$ . In the opposite case of slow and strong fluctuations  $\sigma \geq 2\nu$  this procedure is not valid and a closed master equation for  $R^\tau$  cannot be constructed. Thus, under these conditions other approaches must be used to describe FDMR experiments.

One such approach has been proposed in the general theory of dynamical systems under stochastic influences (see, e.g., Refs. 65 and 73) where, in particular, the powerful method of differentiation formulas has been developed to average the relevant stochastic differential equations. In the Appendix we show that by applying sequentially the differentiation formula for single RT processes,<sup>73</sup>  $d\langle U_k^\tau r^\tau \rangle_{(k)}/d\tau = -2\nu \langle U_k^\tau r^\tau \rangle_{(k)} + \langle U_k^\tau \dot{r}^\tau \rangle_{(k)}$ , where  $\dot{r}^\tau$  is the right-hand part of Eq. (1), one can construct an *exact* system of coupled matrix differential equations

$$\dot{R}^t = DR^t - iF \sum_k^N R^{\{k\}t} + r_0, \quad (16a)$$

$$\dot{R}^{\{k\}t} = (D - 2\nu I)R^{\{k\}t} - iF \sum_{l \neq k}^N R^{\{k,l\}t} - i\sigma_k^2 FR^t, \quad (16b)$$

$$\begin{aligned} \dot{R}^{\{k,l\}t} &= (D - 4\nu I)R^{\{k,l\}t} - iF \sum_{m \neq k,l}^N R^{\{k,l,m\}t} - i\sigma_k^2 FR^{\{l\}t} \\ &\quad - i\sigma_l^2 FR^{\{k\}t}, \end{aligned} \quad (16c)$$

...

$$\begin{aligned} \dot{R}^{\{1,\dots,N\}t} &= (D - 2N\nu I)R^{\{1,\dots,N\}t} \\ &\quad - iF \sum_k^N R^{\{1,\dots,k-1,k+1,\dots,N\}t} \end{aligned} \quad (16d)$$

for the averages  $R^t = \langle r^t \rangle$ ,  $R^{\{k\}t} = \langle U_k^t r^t \rangle$ ,  $R^{\{k,l\}t} = \langle U_k^t U_l^t r^t \rangle$ ,  $\dots$ ,  $R^{\{1,\dots,N\}t} = \langle U_1^t \dots U_N^t r^t \rangle$ . Equations (16a)–(16d) are used below to calculate exactly the average optically detected response  $R_2^t = \langle \rho_{11}^t \rangle$  of a molecule to a MW field and compare it both with experimental data and with approximate calculations.

The total dimensionality of Eqs. (16a)–(16d) for our five-level molecule is  $8 \times 2^N$ ; hence, it increases rapidly with the number  $N$  of the component RT processes. Therefore, from the computational viewpoint, it is desirable to have  $N$  as small as possible. On the other hand, however,  $N$  must be large enough to approximate well the total effect of many

flipping proton spins in the surrounding host crystal to the single triplet spin. Analysis has shown that such a minimum but sufficient number  $N$  of RT processes in the model is determined mainly by the value of the ratio  $\sigma/2\nu$ : the higher the ratio is, the larger must be the number  $N$  of component RT processes in the model. In Sec. III we show that for the investigated Pc+PT system  $\sigma/2\nu \approx 1.4$  and four component processes ( $N=4$ ) are sufficient to fit well the experimental observations within our  $N$  RT model. For this reason exact calculations with Eqs. (16a)–(16d) are restricted in this work to  $N \leq 4$ .

In the Appendix we describe additionally the other more conventional method that can be used to average Eq. (1) over fluctuation histories. The method is known as sudden modulation theory.<sup>24,32–34,74,75</sup> According to this method Eqs. (16a)–(16d) are replaced by Eq. (A10) for so-called “end marginal” averages  $R^{\{\lambda_1, \dots, \lambda_N\}t}$  which are partial averages of the vector  $r^t$  over only those histories of all component processes  $U_k^t$  which end at time  $t$  at some specific value  $U_k = \lambda_k \sigma_k$ , where  $\lambda_k = \text{sgn}(U_k)$  (see also Refs. 76 and 77 for a review and references). It should be stressed that Eq. (A10) is completely equivalent to Eqs. (16a)–(16d) and, in principle, can be used to calculate  $\langle \rho_{11}^t \rangle$ . Note also that the integrodifferential equations (9) can be obtained from Eqs. (16a)–(16d) if one substitutes the formal solution of Eq. (16b) into Eq. (16a). Furthermore, in the limit of a large jump rate  $\nu$  and total variance  $\sigma$ , one recovers the limit of the Bloch equations with pure dephasing rate  $K_{XZ} = \sigma^2/2\nu$ .

If  $k_j^i \ll \nu$ , Eqs. (16a)–(16d) can be simplified significantly. According to Eqs. (16a)–(16d), the averages  $R^{\{k\}t}$ ,  $R^{\{k,l\}t}$ ,  $\dots$ ,  $R^{\{1,\dots,N\}t}$  decay with rates  $2\nu, 4\nu, \dots, 2N\nu \gg k_j^i$  and, as a consequence, it is possible to neglect  $D_K$  in Eq. (2) and replace the matrix  $D$  in Eqs. (16b)–(16d) by  $D_V + D_W$ . Moreover, when  $k_j^i \ll \nu$ , there are two time scales in the problem. The vector  $\tilde{r}^t = (\rho_{XZ}^t, \Delta^t, \rho_{ZX}^t)$  evolves on a time scale  $\sim \tau_c = (2\nu)^{-1}$ , while other elements of  $R^t$  evolve on a time scale  $(k_j^i)^{-1} \gg \tau_c$ . Taking into account that the operator  $F$  acts as a projection operator onto the three-dimensional subspace of  $\tilde{r}^t$ , one finds that, for  $t < (k_j^i)^{-1}$ , one can replace the complete  $8 \times 2^N$  by  $8 \times 2^N$  matrix equations (16a)–(16d) by the  $3 \times 2^N$  by  $3 \times 2^N$  matrix equations

$$\dot{\tilde{R}}^t = -i(\delta S_z + 2WS_x)\tilde{R}^t - iS_z \sum_k^N \tilde{R}^{\{k\}t}, \quad (17a)$$

$$\begin{aligned} \dot{\tilde{R}}^{\{k\}t} &= -i(\delta S_z + 2WS_x - 2i\nu I)\tilde{R}^{\{k\}t} - iS_z \sum_{l \neq k}^N \tilde{R}^{\{k,l\}t} \\ &\quad - i\sigma_k^2 S_z \tilde{R}^t, \end{aligned} \quad (17b)$$

$$\begin{aligned} \dot{\tilde{R}}^{\{k,l\}t} &= -i(\delta S_z + 2WS_x - 4i\nu I)\tilde{R}^{\{k,l\}t} \\ &\quad - iS_z \sum_{m \neq k,l}^N \tilde{R}^{\{k,l,m\}t} \\ &\quad - i\sigma_k^2 S_z \tilde{R}^{\{l\}t} - i\sigma_l^2 S_z \tilde{R}^{\{k\}t}, \end{aligned} \quad (17c)$$

...

$$\begin{aligned} \dot{\tilde{R}}^{\{1, \dots, N\}t} = & -i(\delta S_z + 2WS_x - 2Ni\nu I)\tilde{R}^{\{1, \dots, N\}t} \\ & -iS_z \sum_k^N \tilde{R}^{\{1, \dots, k-1, k+1, \dots, N\}t} \end{aligned} \quad (17d)$$

for the averages  $\tilde{R}^t = \langle \tilde{r}^t \rangle$ ,  $\tilde{R}^{\{k\}t} = \langle U_k^t \tilde{r}^t \rangle$ ,  $\tilde{R}^{\{k,l\}t} = \langle U_k^t U_l^t \tilde{r}^t \rangle$ ,  $\dots$ ,  $\tilde{R}^{\{1, \dots, N\}t} = \langle U_1^t \dots U_N^t \tilde{r}^t \rangle$ , supposing that the other components of vectors  $R^t$ ,  $R^{\{k\}t}$ ,  $R^{\{k,l\}t}$ ,  $\dots$ ,  $R^{\{1, \dots, N\}t}$  are constant on this time scale. Due to the condition  $t < (k_j^i)^{-1}$ , we also are able to omit the inhomogeneous vector  $\tilde{r}_0$  with the components  $(0, -(k_0^X - k_0^Z)/4, 0)$  on right-hand part of Eq. (17a). Equations (17a)–(17d) are especially useful in calculating the transient FDMR response of a molecule to a pulsed MW field (see Sec. III B). Note that analogous theories of optically detected magnetic resonance (ODMR) phenomena have been given in which one considers in detail only two resonant triplet substates with the other states of the molecule serving as population sources or sinks (see, e.g., Ref. 37). Our version, Eqs. (17a)–(17d), differs from previous theories in that we use a stochastic approach and take into account a nonvanishing correlation time for the triplet-substate frequency fluctuations.

### III. APPLICATIONS

The general formalism developed in Sec. II can be used to model both cw and transient experiments. In this paper we

calculate (i) MW-power-broadened FDMR line shapes and (ii) coherent transients such as fluorescence-detected free induction decay and fluorescence-detected two-pulse echoes on single molecules. The theory is used to fit the available experimental data on single Pc molecules in crystalline PT. By considering both time- and frequency-domain measurements, we can understand how triplet spin pure dephasing mechanisms operate in both the time and frequency domains. Preliminary results have been published in Refs. 40–42 along with additional descriptions of experiments in which transient nutation<sup>14</sup> and the second-order correlation function  $g^{(2)}(\tau)$  of the fluorescence intensity have been measured<sup>15</sup> in the Pc+PT system.

#### A. Power-broadened FDMR line shapes

The FDMR line shape is a measure of the average fluorescence intensity as a function of the frequency  $\omega$  of the cw MW field driving the triplet manifold. As was discussed previously this line shape is the convolution of the steady-state homogeneous line shape  $\langle \rho_{11}^{st}(\omega) \rangle$  with the distribution  $P(\bar{\omega}_{XZ})$  of  $X$ - $Z$  transition frequencies:  $I^{st}(\delta) \sim \int d\Delta P(\Delta) \langle \rho_{11}^{st}(\Delta - \delta) \rangle$ .

It is instructive first to calculate the homogeneous line shape  $\langle \rho_{11}^{st}(\omega) \rangle$  when the system is described by the conventional BE's. In this case the *exact* steady-state solution  $\rho_{11}^{st}$  is

$$\rho_{11}^{st}(\delta) = \frac{\rho_{11}^{(0)st}}{1 + \rho_{11}^{(0)st} \frac{B_{xz} u_{mw}}{1 + B_{xz} u_{mw} (1/k_0^X + 1/k_0^Z)} (1/k_0^Z - 1/k_0^X) (k_X^1/k_0^X - k_Z^1/k_0^Z)}, \quad (18)$$

where

$$\rho_{11}^{(0)st} = \frac{1}{2} \frac{4V^2(\Gamma/\tilde{A})}{\Gamma^2 + 4V^2(\Gamma/\tilde{A})(1 + k_X^1/2k_0^X + k_Y^1/2k_0^Y + k_Z^1/2k_0^Z)} \quad (19)$$

is the steady-state population of state 1 when an exactly resonant optical field drives the singlet transition and there is no MW field driving the triplet transitions,

$$B_{xz} u_{mw} = 2W^2 \gamma / (\delta^2 + \gamma^2) \quad (20)$$

is the Einstein coefficient for MW-field-induced transitions,  $\Gamma = \tilde{A}/2 + K_{10}$  is the optical 1-0 transition linewidth with  $\tilde{A} = A + k_X^1 + k_Y^1 + k_Z^1$  and  $K_{10}$  a pure dephasing contribution (recall that for the Pc+PT system  $K_{10} = 0$ ,<sup>50</sup> which is also the case for most other impurity molecules in *crystalline* host matrices), and  $\gamma = (k_0^X + k_0^Z)/2 + K_{XZ}$  is the total linewidth of the  $X$ - $Z$  transition with a pure dephasing contribution  $K_{XZ}$  resulting from  $\delta$ -correlated (in the Bloch case) frequency fluctuations  $U^t$ .

Equations (18)–(20) describe a homogeneous FDMR line shape  $\rho_{11}^{st}(\delta)$  that is symmetric about  $\delta = 0$ . The population

$\rho_{11}^{st}(\delta)$  decreases from its value  $\rho_{11}^{(0)st}$  at large MW field detunings  $\delta$  to a minimum  $\rho_{11}^{st}(\delta = 0)$  at  $\delta = 0$ . The relative decrease at line center compared with the line wings in the case of strong MW fields,  $2W \gg \gamma$ , is

$$\begin{aligned} E &= [\rho_{11}^{(0)st} - \rho_{11}^{st}(\delta = 0)] / \rho_{11}^{(0)st} \\ &= \left[ 1 + \frac{1}{\rho_{11}^{(0)st}} \frac{(1/k_0^X + 1/k_0^Z)}{(1/k_0^Z - 1/k_0^X)(k_X^1/k_0^X - k_Z^1/k_0^Z)} \right]^{-1}. \end{aligned} \quad (21)$$

The quantity  $E$  can be thought of as a measure of the effectiveness of the FDMR technique. In the case of the Pc+PT pair, using ISC rates from Table 1 of Ref. 15, one finds  $E \sim 0.27$ .

It is worthwhile pointing out that, according to Eqs. (18) and (21), the FDMR effect is absent if (i)  $k_X^1/k_0^X = k_Z^1/k_0^Z$  or (ii)  $k_0^X = k_0^Z$ . In other words, if the populating and depopulat-

ing rates of the two triplet substates of the molecule are proportional to each other or if their lifetimes are equal, the application of a MW field that couples these two substates does not influence the population of state 1. If  $k_X^1/k_0^X = k_Z^1/k_0^Z$ , then the populations  $\rho_{XX}^{(0)st} = (k_X^1/k_0^X)\rho_{11}^{(0)st}$  and  $\rho_{ZZ}^{(0)st} = (k_Z^1/k_0^Z)\rho_{11}^{(0)st}$  are equal in the absence of an applied MW field, and this relationship is unchanged after the MW field is switched on. If  $k_0^X = k_0^Z$ , the MW field results in a specific redistribution of the populations in the five-level system, but leaves the state 1 population unchanged.

The half width  $h$  (half width at half height of the dip) of the line shape  $\rho_{11}^{st}(\delta)$ , calculated from Eq. (18), is given by

$$h^2 = \gamma^2 + 2W^2\gamma \left[ \frac{1}{k_0^Z} + \frac{1}{k_0^X} + \rho_{11}^{(0)st} \left( \frac{1}{k_0^Z} - \frac{1}{k_0^X} \right) \left( \frac{k_X^1}{k_0^X} - \frac{k_Z^1}{k_0^Z} \right) \right]. \quad (22)$$

In weak MW fields,  $2W \ll \gamma$ , the line shape (18) is Lorentzian with half width  $\gamma$ . In this limit, the total line shape  $I^{st}(\delta) \sim \int d\Delta P(\Delta)\rho_{11}^{st}(\Delta - \delta)$  follows approximately the shape of the  $X$ - $Z$  transition frequency distribution  $P(\bar{\omega}_{XZ})$  evaluated at  $\bar{\omega}_{XZ} = \delta$ ,

$$I^{st}(\delta) \sim \rho_{11}^{(0)st} \left[ 1 - 4\pi W^2 \rho_{11}^{(0)st} \left( \frac{1}{k_0^Z} - \frac{1}{k_0^X} \right) \left( \frac{k_X^1}{k_0^X} - \frac{k_Z^1}{k_0^Z} \right) P(\delta) \right], \quad (23)$$

provided that  $\gamma$  is much less than the frequency width of this distribution. In the opposite limit of strong MW fields, Eq. (22) gives a half width  $h$  that grows linearly with the MW Rabi frequency  $2W$ . If  $2W$  exceeds the width  $H_p$  of the distribution  $P(\Delta)$  so that the MW field saturates all frequencies in the distribution, the line shape  $I^{st}(\delta)$  is identical to the homogeneous line shape, Eq. (18). If  $k_0^X \gg k_0^Z$ ,  $k_X^1/k_0^X \gg k_Z^1/k_0^Z$ , which is the case for the Pc+PT pair,<sup>15</sup> the power-broadened FDMR line width is given approximately by

$$h \approx 2W \sqrt{\frac{\gamma}{2k_0^Z} \left( 1 + \rho_{11}^{(0)st} \frac{k_X^1}{k_0^X} \right)}. \quad (24)$$

It should be pointed out that due to the presence of the small rate  $k_0^Z$  in the denominator of Eq. (24),  $dh/dW$  is large for the Pc+PT system.

As was discussed in the Introduction, the BE's fail to give a correct description of power broadening in systems with slow frequency fluctuations. Therefore Eqs. (18) and (22) are expected to be inconsistent with experimental data on MW-power-broadened FDMR line shapes for single guest molecules in organic host matrices such as the Pc+PT system. For this reason we extend the above BE-based calculations of the FDMR line shape to include non-Markovian triplet spin dephasing. It is assumed that  $\nu \gg k_j^i$ , allowing us to use Eq. (10) as the starting point of our calculations, with the kernel  $L^{t-\tau} = F e^{D(t-\tau)} F$  approximated by Eq. (13). Furthermore, we factor the correlation function  $\langle U^t U^\tau r^\tau \rangle \approx \langle U^t U^\tau \rangle R^\tau$ , which is valid for a single, symmetric RT process. The steady-state solution of the equations obtained after these simplifications is  $R^{st} = -(D - \bar{L})^{-1} r_0$ , where the matrix  $D$  is determined by Eq. (2) and

$$\bar{L} = \sigma^2 \int_0^\infty dx L^x e^{-\nu\tau} = \begin{pmatrix} Z_{5,5} & Z_{3,5} & & \\ & F_1 & 0 & F_2 \\ Z_{5,3} & 0 & 0 & 0 \\ & F_2 & 0 & F_1^* \end{pmatrix}. \quad (25)$$

The factors

$$F_1 = \frac{\sigma^2}{2\nu} \left[ \frac{s^2}{2} + \left( c^2 + \frac{s^2}{2} - i \frac{\delta}{2\nu} \right) \frac{4\nu^2}{4\nu^2 + \Omega^2} \right], \quad (26a)$$

$$F_2 = \frac{\sigma^2}{4\nu} \frac{4W^2}{4\nu^2 + \Omega^2} \quad (26b)$$

are integrals over time of the product of the functions  $f_i^t$  in Eqs. (12a) and (12b) with the correlation function  $\langle U^t U^0 \rangle = \sigma^2 \exp(-2\nu t)$  of dephasing fluctuations  $U^t$ . Recall that  $s = 2W/\Omega$ ,  $c = \delta/\Omega$ , and  $\Omega = (\delta^2 + 4W^2)^{1/2}$ .

After some algebra one can calculate for this case the steady-state population  $\langle \rho_{11}^{st}(\delta) \rangle = R_2^{st}(\delta)$  in explicit form and find that it is again given by the expression (18) but with the Einstein coefficient  $B_{xz} u_{mw}$  replaced by

$$B_{xz} u_{mw} = 2W^2 \frac{(k_0^X + k_0^Z)/2 + (\text{Re } F_1 - F_2)}{|i\delta + (k_0^X + k_0^Z)/2 + F_1|^2 - F_2^2}. \quad (27)$$

This equation reduces to Eq. (20) in the limit of  $\delta$ -correlated fluctuations [ $\sigma, \nu \rightarrow \infty, \lim(\sigma^2/2\nu) = K_{XZ}$ ] when the functions (26a) and (26b) become  $F_1 \rightarrow K_{XZ}$  and  $F_2 \rightarrow 0$ . On the contrary, if the correlation time  $\tau_c = (2\nu)^{-1}$  is nonvanishing, the presence in Eq. (27) of the MW-field-dependent functions  $F_i$  leads to differences between the homogeneous FDMR line shape  $\langle \rho_{11}^{st}(\delta) \rangle$  evaluated using Eq. (27) with the BE line shape evaluated using Eq. (20). In particular, in strong MW fields,  $W \gg \nu$ , when both functions  $F_i$  are approximately equal to  $s^2\sigma^2/4\nu$ , one can obtain from Eq. (27) an equation similar to Eq. (20) but with the linewidth  $\gamma$  determined now as  $\gamma = (k_0^X + k_0^Z)/2$ , i.e., consisting of only the triplet-state-lifetime-limited part of the previous total linewidth  $\gamma = (k_0^X + k_0^Z)/2 + K_{XZ}$ . In turn, the FDMR line width  $h$  can now be calculated from Eq. (20) with the substitution  $\gamma \rightarrow (k_0^X + k_0^Z)/2$ . Thus, when  $W \gg \nu$  the contributions from triplet resonance frequency fluctuations are canceled completely and the MW-power-broadened FDMR line becomes much narrower in comparison with the BE predictions. It is shown below that for the Pc+PT system this "field-narrowing effect"<sup>78</sup> is very pronounced:  $\sqrt{1 + 2K_{XZ}/k_0^Z} \sim 30$ .

If the fluctuations  $U^t$  are modeled by an  $N$  RT model, an analytical expression for the homogeneous FDMR line shape can no longer be obtained. Instead, one must turn to a numerical solution of Eqs. (16a)–(16d). Below we calculate  $\langle \rho_{11}^{st}(\delta) \rangle$  for a Pc+PT pair, using values for  $k_j^i, A, V, \Gamma_{10}$  given in Table 1 of Ref. 15. For the jump rate of the component RT processes  $U_k^t$ , we take the value  $\nu/2\pi = 30$  kHz, which is the typical average proton spin flip-flop rate in Pc+PT at liquid helium temperature.<sup>17,79</sup> We assume also that the fluctuations  $U^t$  are slow,  $\sigma^2/4\nu^2 \geq 1$ , and that the processes  $U_k^t$  have same variances  $\sigma_k = \sigma/\sqrt{N}$ . Figures 2(a)–2(c) show the results of calculations made using the value

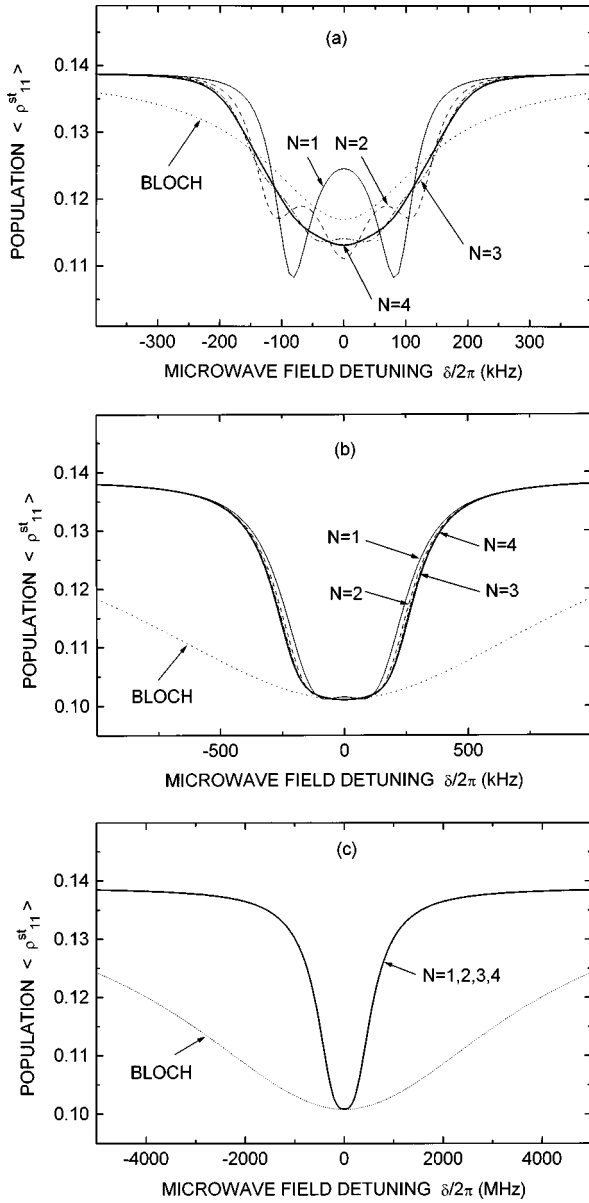


FIG. 2. Homogeneous FDMR line shapes  $\langle \rho_{11}^{st}(\omega) \rangle$  calculated using  $N$  RT models with  $N=1,2,3,4$  for  $\nu/2\pi=30$  kHz,  $\sigma/2\pi=85$  kHz for different values of the MW Rabi frequency: (a)  $2W/2\pi=6$  kHz (case  $2W < \nu < \sigma$ ), (b)  $2W/2\pi=55$  kHz (case  $\nu < \sigma < 2W$ ), and (c)  $2W/2\pi=200$  kHz (case  $\nu < \sigma < 2W$ ). Dotted curves show the Bloch equation (BE) predictions using  $K_{XZ}/2\pi=100$  kHz.

$\sigma/2\pi=85$  kHz which have been determined by a best fit of the experimental data for Pc molecules in crystalline PT. It should be noted that, owing to the condition  $k_j^i \ll \nu$  which is well satisfied for Pc+PT, all results are practically indistinguishable from those obtained using the simplified version of Eqs. (16b)–(16d) with the matrix  $D$  replaced by  $D_V + D_W$ . Additionally, for  $N=1$  the exact calculations coincide with those predicted by Eqs. (18) and (27).

The homogeneous line shape  $\langle \rho_{11}^{st}(\delta) \rangle$  is shown in Fig. 2(a) in the limit of weak MW fields,  $2W \ll 2\nu \leq \sigma$ . For small values of  $N$ , there are peak-shaped structures resulting from individual MW field resonances with fluctuation-shifted frequencies  $\omega_{XZ}^{[\lambda_k]} = \omega_{XZ} + \sum \lambda_k \sigma_k$  ( $[\lambda_k] = \lambda_1, \dots, \lambda_N; \lambda_k =$

$\pm 1$ ) of the  $X$ - $Z$  transition which are well separated in this case. For higher  $N$ , in accordance with the central limit theorem (see, e.g., Ref. 65), the line shape approaches the Gaussian limit  $\sim \rho_{11}^{(0)st} [1 - C_G \exp(-\delta^2/2\sigma^2)]$  with half width  $h = \sigma \sqrt{2 \ln 2} \sim \sigma$ . Note that with the parameter values peculiar to the Pc+PT system four-component processes ( $N=4$ ) in the model provide a good approximation for the above Gaussian line shape. Further increasing the number  $N$  of the component RT processes (at fixed variance  $\sigma/2\pi=85$  kHz) does not change essentially the homogeneous line shape calculated with  $N=4$ . For the slow modulation case under consideration, the line shape depends only slightly on the jump frequency  $\nu$ . Figure 2(b) demonstrates that these spectral peaks practically disappear at moderate MW field power,  $2\nu < 2W \leq \sigma$ . Note also in Fig. 2(b) that the linewidth is approximately twice that of the low-field result at this moderate MW field intensity. A further increase in MW field Rabi frequency ( $2\nu < \sigma \leq 2W$ ) results in the total disappearance of the structure [Fig. 2(c)], and for  $\sigma \leq 2W$  the FDMR linewidth  $h$  is given by Eq. (22) at any  $N$ , indicating the complete suppression of induced dephasing associated with  $N$  RT processes by the MW field. For comparison purposes we also show in Figs. 2(a)–2(c) the line shapes calculated in the motional narrowing limit [ $\sigma, \nu \rightarrow \infty, \lim(\sigma^2/2\nu) = K_{XZ}$ ] on the basis of the BE (18), setting  $K_{XZ}/2\pi=100$  kHz equal to the low-power Gaussian-limit linewidth  $h = \sigma \sqrt{2 \ln 2}$ . One can conclude from the figures that homogeneous power-broadened FDMR line shapes predicted by BE's are much broader than the corresponding slow-modulation-induced line shapes.

Now we calculate, in terms of the  $N$  RT model, the power-broadened inhomogeneous FDMR line shape  $I^{st}(\delta) \sim \int d\Delta P(\Delta) \langle \rho_{11}^{st}(\Delta - \delta) \rangle$ . For the  $X$ - $Z$  transition of Pc in PT the inhomogeneous FDMR line has been observed<sup>12,13</sup> at low microwave power to be strongly asymmetric with a sharp low-frequency edge, having half width at half maximum (HWHM)  $\sim 200$  kHz, and a slowly decreasing high-frequency tail extending for  $\sim 10$  MHz. The full width (at half maximum level) of the distribution is approximately 5 MHz. In principle, the distribution  $P(\bar{\omega}_{XZ})$  can be calculated from first principles following the method described in Ref. 54 and using the hfi-tensor parameters for the Pc+PT pair determined in Ref. 81. Such calculations, performed previously,<sup>15</sup> show that, owing to the large number of protons ( $2^{14}$ ) in Pc molecules, this distribution is dense and in reasonable agreement with the low-power experimental FDMR line shape, Eq. (23). For these reasons and to simplify the calculations, we will use in our further analysis a simple analytical approximation for the distribution  $P(\Delta)$ :  $P(\Delta)=0$  for  $\Delta < 0$  and  $P(\Delta) = (1/\Delta_0) \exp(-\Delta/\Delta_0)$  for  $\Delta \geq 0$  with  $\Delta_0/2\pi=4.7$  MHz. Calculations of the low-power inhomogeneous line shape  $I^{st}(\delta)$  using the above model distribution agree well with the experimental data, Fig. 3(a). Furthermore, from these calculations we conclude that the half width of the sharp edge of the low-power line shape is *twice* the homogeneous linewidth  $h$ , which can be understood easily if one recalls the analogous result, well known in nonlinear spectroscopy, that the low-power limit of the half width of the spectral hole burned due to saturation in a broad inhomogeneous distribution is also equal to *twice* the

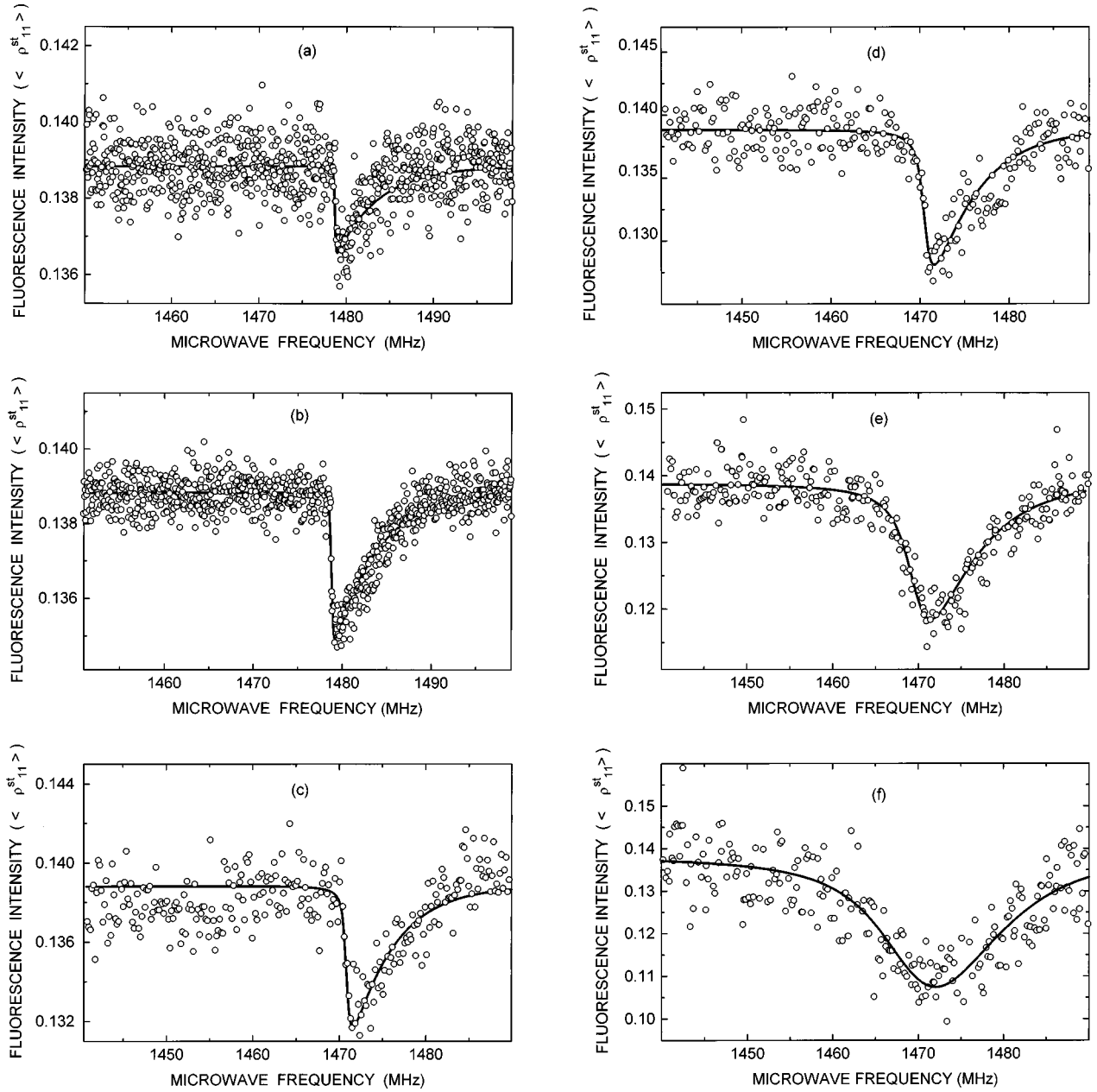


FIG. 3. Inhomogeneous FDMR line shapes  $\bar{\rho}_{11}^{st}(\omega)$  calculated using the 1 RT model at  $\nu/2\pi=30$  kHz,  $\sigma/2\pi=85$  kHz for different values of the MW field Rabi frequency: (a)  $2W=0.09\times 10^6$  s $^{-1}$ , (b)  $2W=0.27\times 10^6$  s $^{-1}$ , (c)  $2W=0.8\times 10^6$  s $^{-1}$ , (d)  $2W=1.6\times 10^6$  s $^{-1}$ , (e)  $2W=5\times 10^6$  s $^{-1}$ , and (f)  $2W=15\times 10^6$  s $^{-1}$  in comparison with experimental data for X-Z transitions of a single Pc molecule in a PT crystal.

homogeneous linewidth (see, e.g., Ref. 9). Therefore, we choose the value  $\sigma/2\pi=85$  kHz ( $=200/2\sqrt{2\ln 2}$  kHz) for the parameter  $\sigma$  of our  $N$  RT model. The above model distribution  $P(\Delta)$  has been used to calculate power-broadened inhomogeneous line shapes for increased values of the MW field Rabi frequencies  $2W$ . Figures 3(b)–3(f) show the results of these calculations in comparison with experimental data. The experimental values of  $2W$ , which were rather large so that the models with different numbers  $N$  of RT processes (at fixed  $\nu$  and  $\sigma$ ) resulted practically in the same homogeneous line shapes, made it possible to restrict calculations to the simplest 1 RT model only. Thus, the analytical expressions (18), (20), and (27) for the homogeneous line shape are well suited for the Pc+PT system. The experimen-

tal data, which give the MW field frequency dependence of the average number of fluorescence photon counts plus any stray light, have been modified by proper scaling and shifting along the y axis to provide a best fit to the calculated line shapes  $I^{st}(\delta)$ . One can see from the Figs. 3(b)–3(f) that this fitting procedure works well for all experimental power-broadened line shapes. Note that even at very high MW field power [Fig. 3(f)], when the MW Rabi frequency  $2W=15\times 10^6$  s $^{-1}$  is comparable with FWHM  $H_p$  of the distribution  $P(\Delta)$  ( $H_p\sim 2\pi\times 5\times 10^6$  s $^{-1}$ ), the line shape  $I^{st}(\delta)$  has a width that is power broadened by a factor of  $\sim 4$  times only. Finally, in Fig. 4 we show a summary of Figs. 3(a)–3(f) with respect to the MW Rabi frequency dependence of the power-broadened linewidth (FWHM). We also show in Fig. 4 the

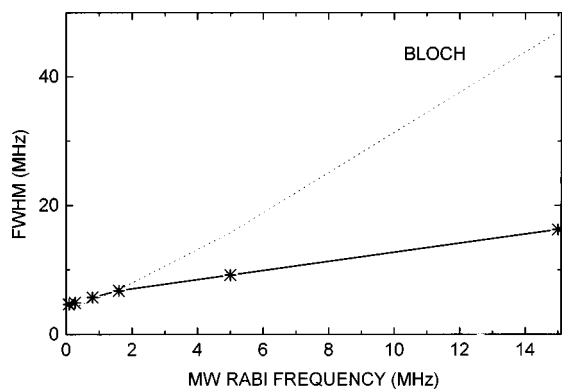


FIG. 4. The MW field Rabi frequency dependence of inhomogeneous FDMR linewidth (FWHM) of the line shapes shown in Figs. 3(a)–3(f) in comparison with experimental data (asterisks) for a single Pc molecule in PT crystal and with BE predictions with  $K_{XZ}/2\pi = 100$  kHz (dotted line).

pronounced disagreements of BE-based calculations (with  $K_{XZ}/2\pi = 100$  kHz) of the FDMR linewidths with the experimental (asterisks) values and  $N$  RT-model-based calculations.

### B. FDMR transients

In the previous subsection we have considered the frequency-domain manifestations of slow fluctuations of a triplet spin frequency, resulting from host molecule proton spin dynamics, in the homogeneous FDMR line shape. It was shown that direct observation of the homogeneously broadened FDMR line shape of a *single* chromophore molecule is difficult to achieve, owing to inhomogeneous broadening imposed by different configurations of Pc molecule proton spins, all of which are sampled during the long duration of FDMR experiment. For this reason frequency-domain FDMR experiments can provide only an estimate of the variance  $\sigma$  of frequency fluctuations  $U^i$ , obtained by measuring the width of the sharp edge of the experimental asymmetric FDMR line. Attempts to determine the homogeneous linewidth by increasing the MW field power and to extract from the linewidth information concerning mechanisms underlying triplet spin pure dephasing fail, as a result of the suppression of these mechanisms by a strong MW field.

To overcome the above difficulties of measuring the homogeneous linewidth of triplet-state chromophore molecules in organic host crystals it has been proposed in Ref. 17 to use time-domain FDMR techniques which have been developed in conventional ODMR spectroscopy to study the coherence decay processes of ensembles of triplet spins (see, e.g., Refs. 36–39, 80, and 82) in single-molecule spectroscopy. The observations of the FDMR Hahn echo<sup>17,83</sup> (FDMR HE) for single Pc molecules in PT crystal have demonstrated that FDMR spectroscopy can provide information concerning the rates of triplet spin pure dephasing in mixed molecular crystals and their variations among different chromophore molecules. Below we extend the BE-based analysis of the FDMR HE (Ref. 17) to describe the triplet spin coherence decay due to slow fluctuations  $U^i$  and to study their manifestations in different transient FDMR phenomena.

During transient FDMR experiments on single molecules the molecule is repeatedly subjected to a specific sequence of

MW field pulses with the total time of the experiment  $T_{\text{expt}}$  much larger than the duration  $T_{\text{seq}}$  of a single MW pulse sequence. Each pulse sequence acting on the molecule can be thought of as a single transient experiment. Some MW field pulses in the sequence are designed to build up the coherence of resonant triplet spin substates  $X$  and  $Z$  or to modify it in a predetermined way. The fluctuations of the transition  $X$ - $Z$  frequency due to host proton spin dynamics introduce shifts  $\Delta\phi = \int dx U^x$  into the relative phase of these states. Coherence between the substates can be probed, within the FDMR technique, by applying an additional  $\pi/2$  MW pulse as the final pulse in the sequence. The function of this final probe MW pulse is to convert coherence into a population difference of substates  $X$  and  $Z$  which is detected using the FDMR technique.

As was discussed previously, a single molecule undergoes quantum jumps between its five states which are accompanied by absorption or emission of optical photons in the singlet-singlet channel or by emission of phonons in ISC transitions to and from triplet substates. Due to the long-time scale character of the FDMR technique, the observables in transient FDMR experiments represent averages over ensembles of single transient experiments. Therefore, from a theoretical viewpoint, one can calculate first the transient response of a molecule during a single FDMR experiment and then average the results as necessary. First, it is necessary to average over the initial states of the molecule just before the arrival of the leading MW pulse in a sequence. In fact, the MW pulse can strike a molecule when it is in any one of its five states (singlet states  $S_0, S_1$  or triplet substates  $X, Y, Z$ ), with the relative probability to be in these states given by diagonal elements of the molecule's density matrix. Evidently, MW field pulses influence the molecule only if it is in one of the MW-field-coupled substates  $X$  or  $Z$ . Experimentally, the repetitive sequences of MW field pulses are separated by a delay time  $T_{\text{del}}$  which is chosen to be sufficiently large to ensure that, by the end of this time, the density matrix for a molecule is equal to the steady-state density matrix. This implies that different single transient experiments can be thought of as independent. The molecular state just before each specific single transient experiment is described by the steady-state density matrix  $\rho_{ij}^{(o)st}$  of a molecule subjected to a cw optical field and to the ISC transitions with no MW field. Second, one must average over the phase shifts  $\Delta\phi$  introduced by fluctuations  $U^i$  in single transient experiments. These shifts are different due to different histories of fluctuations  $U^i$  during single experiments. When averaged over ensembles of many single experiments performed during total transient experiment time  $T_{\text{expt}}$ , these phase shifts manifest themselves as a pure dephasing of the triplet spin transition  $X$ - $Z$ . Furthermore, during  $T_{\text{expt}}$  the molecule is subjected to many cycles  $S_0 \rightarrow S_1 \rightarrow \dots \rightarrow T \rightarrow S_0$ , changing many times its proton spin configuration so that all possible triplet spin transition frequencies are sampled according to the probability distribution  $P(\bar{\omega}_{XZ})$ . Thus, a final average over the inhomogeneous distribution  $P(\bar{\omega}_{XZ})$  must be performed. Note, however, that the above-mentioned averaging over initial molecular states is applicable to describe only the simplest version of transient FDMR experiments when there is no synchronization of

MW pulses with the molecular state. More elaborate versions of experiments can involve so-called “triggering” of MW pulses<sup>15</sup> by fluorescence photons, that is, synchronization of the MW field switching with the appearance (or disappearance) of fluorescence photon bunches in the singlet channel which are correlated with molecular jumps out of or into the triplet substates  $T$ . Calculations of average molecular transient responses for such “triggered” transient FDMR experiments require one to use an initial density matrix  $\tilde{\rho}_{ij}^{(0)trigg}$  that correlates with the timing of the trigger pulse. Additionally, as was pointed out previously in the case of transient FDMR experiments on samples with deuterated (or substituted) molecules, a modified inhomogeneous distribution  $P(\bar{\omega}_{XZ})$  must be used. In particular, the deuterated Pc/PT crystal is not expected to exhibit a normal echo signal since there is no inhomogeneous distribution of frequencies  $\bar{\omega}_{XZ}$ .<sup>17</sup>

Now we are in a position to proceed to a formulation of a stochastic theory of coherent transient FDMR phenomena on single molecules. Hereafter we restrict ourselves with discussing (i) the fluorescence-detected free induction decay (FDMR FID) after a  $\pi/2$  MW pulse, corresponding to the sequence  $\pi/2-\tau_d-\pi/2$ , and (ii) the fluorescence-detected two-pulse Hahn echo (FDMR HE), corresponding to the sequence  $\pi/2-\tau_{d1}-\pi-\tau_{d2}-\pi/2$ . Both of these transient phenomena are sensitive to pure dephasing mechanisms and therefore they can be used to study them. The terms “ $\pi/2$  and  $\pi$  MW pulses” mean, as usual, that the MW pulses have the Rabi frequencies  $2W_{\pi/2}, 2W_{\pi}$  and durations  $\tau_{\pi/2}, \tau_{\pi}$  satisfying the relations  $2W_{\pi/2}\tau_{\pi/2} = \pi/2$ ,  $2W_{\pi}\tau_{\pi} = \pi$ . Since the typical duration of a single transient experiment ( $\sim$  triplet spin coherence decay time) is short in comparison with the lifetimes  $(k_0^{X(Z)})^{-1}$  of triplet sublevels  $X$  and  $Z$ , it is possible first to simplify matters by supposing that the MW pulse sequence influences only the  $X$ - $Z$  transition with other states of the five-level molecule retaining their steady-state values, described by the density matrix  $\rho_{ij}^{(0)st}$ . With this simplification the effect of the MW pulse sequence on the  $X$ - $Z$  transition can be calculated using the reduced two-level system description. As was discussed previously the two-level system consisting of triplet sublevels  $X$  and  $Z$  is described on short-time scale  $t \ll (k_i^j)^{-1}$  by the three-dimensional vector  $\tilde{r}^t$  which obeys Eq. (8). The initial condition for this equation is  $\tilde{r}^t = \tilde{r}^{(0)st}$ , where the steady-state solution  $\tilde{r}^{(0)st}$  has components  $(0, \Delta^{(0)st}, 0)$ . The population difference  $\Delta^{(0)st} = (\rho_{XX}^{(0)st} - \rho_{ZZ}^{(0)st})/2$  is approximately equal to 0.2129 in the case of Pc+PT. The transient stochastic response  $\tilde{r}^{T_{seq}}$  of a single triplet spin to a single MW pulse sequence of total duration  $T_{seq}$ , calculated using Eq. (8), must be averaged over fluctuation histories  $U^t$  to obtain  $\tilde{R}^{T_{seq}} = \langle \tilde{r}^{T_{seq}} \rangle$ . It is the dependence of the component  $\langle \Delta^{T_{seq}} \rangle$  of the vector  $\tilde{R}^{T_{seq}}$  on  $T_{seq}$  that contains information about the triplet spin dephasing process that can be extracted using the FDMR technique. We proceed to calculate  $\langle \Delta^{T_{seq}} \rangle$  for the above two FDMR transients.

Supposing the  $\pi/2$  and  $\pi$  MW pulses to be very short and strong so that their Rabi frequencies  $2W_{\pi/2}$  and  $2W_{\pi}$  are much larger than all detunings  $\delta$  in the distribution  $P(\delta)$  and the variance  $\sigma$  of fluctuations  $U^t$ , one can neglect  $\delta$  and  $U^t$

in Eq. (8). In this limit, the effects of  $\pi/2$  and  $\pi$  MW pulses on the triplet subspace is described by the matrices

$$G_{\pi/2} = \exp\{-i\pi S_x/2\}, G_{\pi} = \exp\{-i\pi S_x\}. \quad (28)$$

Between MW pulses the triplet spin is influenced by fluctuations  $U^t$  only and its free evolution from  $t'$  to  $t''$  is described, in the Schrödinger representation, by the matrix

$$G_U = \exp\{-iS_z[\omega_{XZ}(t'-t'') + \Delta\phi^{t',t''}]\}, \quad (29)$$

where  $\Delta\phi^{t',t''} = \int_{t'}^{t''} dx U^x$  is the change in relative phase of states  $X$  and  $Z$  during the time interval  $t' - t''$ . Using Eqs. (28) and (29) one finds that  $\langle \Delta^{T_{seq}} \rangle$  at the end  $T_{seq}$  of MW pulse sequences (i) and (ii) is given by

(i) FDMR FID ( $T_{seq} = 2\tau_{\pi/2} + \tau_d \approx \tau_d$ ):

$$\langle \Delta_{FID}^{T_{seq}} \rangle \approx -\Delta^{(0)st} \text{Re}\{\exp(-i\delta\tau_d)\Psi_{FID}^{\tau_d}\}; \quad (30a)$$

(ii) FDMR two-pulse Hahn echo ( $T_{seq} = 2\tau_{\pi/2} + \tau_{\pi} + \tau_{d1} + \tau_{d2} \approx \tau_{d1} + \tau_{d2}$ ):

$$\langle \Delta_{HE}^{T_{seq}} \rangle \approx \Delta^{(0)st} \text{Re}\{\exp[-i\delta(\tau_{d1} - \tau_{d2})]\Psi_{HE}^{\tau_{d1}, \tau_{d2}}\}, \quad (30b)$$

where

$$\Psi_{FID}^t = \left\langle \exp\left\{-i \int_0^t dx U^x\right\}\right\rangle, \\ \Psi_{HE}^{t_1, t_2} = \left\langle \exp\left\{-i \int_0^{t_1} dx U^x + i \int_{t_1}^{t_1+t_2} dx U^x\right\}\right\rangle \quad (31)$$

are the well-known characteristic functionals describing the FI and HE decays when one uses a stochastic description of dephasing.<sup>70</sup> In the BE limit both of them are simple exponentials:  $\Psi_{FID}^t = \exp(-K_{XZ}t)$ ,  $\Psi_{HE}^{t_1, t_2} = \exp(-2K_{XZ}t)$ . In the general case their decays are nonexponential. Therefore, the dependence of these functionals on delay time provides a measure of pure dephasing processes which can be monitored using the FDMR technique as changes in fluorescence intensity after termination of the MW pulse sequence.

To calculate these changes one needs to construct first the eight-dimensional vector  $R^{T_{seq}}$  describing the complete five-level system just after the MW pulse sequence. This vector is obtained from  $\tilde{R}^{T_{seq}}$  by adding the five steady-state components  $\rho_{ij}^{(0)st}$  which have been supposed to be unchanged during the time  $T_{seq}$  to arrive at the complete vector  $R^{T_{seq}}$ :  $R^{T_{seq}} = (\rho_{10}^{(0)st}, \rho_{11}^{(0)st}, \rho_{00}^{(0)st}, \rho_{01}^{(0)st}, \rho_{YY}^{(0)st}, \langle \rho_{XZ}^{T_{seq}} \rangle, \langle \Delta^{T_{seq}} \rangle, \langle \rho_{ZX}^{T_{seq}} \rangle)$ . The vector  $R^{T_{seq}}$  serves as the initial condition to calculate subsequent changes in the average fluorescence intensity, obtained from a solution of Eq. (1) with no MW field. At a time  $\theta$  following the MW field sequence, the molecular density matrix is equal to

$$R^{T_{seq}+\theta} = \exp\{(D_V + D_K)\theta\}[R^{T_{seq}} - R^{(0)st}] + R^{(0)st}, \quad (32)$$

and, for the component of interest  $R_2^{T_{seq}+\theta} = \langle \rho_{11}^{T_{seq}+\theta} \rangle$ , one finds

$$\langle \rho_{11}^{T_{seq}+\theta} \rangle = \Theta(\theta)(\langle \Delta^{T_{seq}} \rangle - \Delta^{(0)st}) + \rho_{11}^{(0)st}, \quad (33)$$

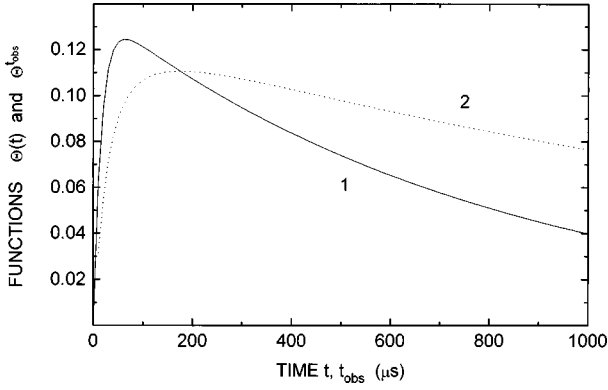


FIG. 5. Functions  $\Theta(t) = \{\exp[(D_V + D_K)t]\}_{27}$ , Eq. (34), curve 1, and  $\Theta^{t_{obs}} = \int_0^{t_{obs}} dt \Theta(t) / t_{obs}$ , curve 2, calculated for parameter values typical of the Pc+PT system.

where  $\Theta(\theta)$  is the 2-7 element of the matrix exponential:

$$\Theta(\theta) = \{\exp[(D_V + D_K)\theta]\}_{27}. \quad (34)$$

The function  $\Theta(\theta)$  calculated for the Pc+PT system is shown in Fig. 5 as curve 1. Relative changes  $\Delta I^\theta$  in the time-dependent average fluorescence intensity  $\langle I^\theta \rangle$  now can be defined as

$$\begin{aligned} \Delta I^\theta &= (I^{(0)st} - \langle I^\theta \rangle) / I^{(0)st} \\ &= 1 - \langle \rho_{11}^{T_{seq} + \theta} \rangle / \rho_{11}^{(0)st} \\ &= \Theta(\theta) (\Delta^{(0)st} - \langle \Delta^{T_{seq}} \rangle) / \rho_{11}^{(0)st}, \end{aligned} \quad (35)$$

which, taking account Eqs. (30a) and (30b), result in the following expressions:

$$\begin{aligned} \Delta I_{FID}^\theta(\tau_d) &= \Theta(\theta) (\Delta^{(0)st} / \rho_{11}^{(0)st}) \\ &\quad \times \{1 + \text{Re}[\exp(-i\delta\tau_d) \Psi_{FID}^{\tau_d}]\}, \end{aligned} \quad (36a)$$

$$\begin{aligned} \Delta I_{HE}^\theta(\tau_{d1}, \tau_{d2}) &= \Theta(\theta) (\Delta^{(0)st} / \rho_{11}^{(0)st}) \\ &\quad \times (1 - \text{Re}\{\exp[-i\delta(\tau_{d1} - \tau_{d2})] \Psi_{HE}^{\tau_{d1}, \tau_{d2}}\}) \end{aligned} \quad (36b)$$

for the FDMR FID and FDMR HE, respectively.

To be able to compare the calculated relative changes in fluorescence intensity after FID and HE sequences with experimental observations one needs additionally to integrate Eqs. (36a) and (36b) over  $\delta$  with the inhomogeneous distribution  $P(\delta)$ . Assuming as previously the distribution  $P(\delta) = (1/\Delta_0) \exp(-\delta/\Delta_0)$  ( $\delta \geq 0$ ) with the width  $\Delta_0$  one can show easily that the integration results in the replacement of the oscillating exponentials  $\exp(-i\delta\tau_d)$  and  $\exp[-i\delta(\tau_{d1} - \tau_{d2})]$  by the Lorentzians  $1/(1 + \tau_d^2 \Delta_0^2)$  and  $1/[1 + (\tau_{d1} - \tau_{d2})^2 \Delta_0^2]$ , respectively. In the case of Eq. (36a) the decay behavior of the FDMR FID signal is determined by both the inhomogeneous distribution width  $2\pi\Delta_0$  and the ‘‘effective’’ homogeneous pure dephasing rate, i.e., the characteristic decay rate of the functional  $\Psi_{FID}^{\tau_d}$ . Typically the decay due to the inhomogeneous distribution dominates that of pure dephasing. As a consequence, the FDMR FID phenomena are practically insensitive to homogeneous pure dephas-

ing (it should be noted, however, that FDMR FID experiments on deuterated samples could, in principle, provide a method to study homogeneous dephasing alone due to a reduction of inhomogeneous broadening in this case). In contrast, it follows from Eq. (36b) that the FDMR HE provides the possibility to measure the true homogeneous pure dephasing decay rate by choosing the HE MW pulse sequence with equal delay times  $\tau_{d1} = \tau_{d2} = \tau_d$  to cancel the influence of inhomogeneous broadening. The decay is described by the  $\tau_d$  dependence of the functional  $\Psi_{HE}^{\tau_d, \tau_d}$ . Within the  $N$  RT model for fluctuations  $U^t$  this functional can be calculated exactly in explicit form:<sup>65</sup>

$$\begin{aligned} \Psi_{HE}^{\tau_d, \tau_d} &= \exp(-2N\nu\tau_d) \prod_{k=1}^N \left\{ \frac{\sigma_k^2}{\mu_k^2} + \frac{\nu}{\mu_k} \left[ \sin(2\mu_k\tau_d) \right. \right. \\ &\quad \left. \left. - \frac{\nu}{\mu_k} \cos(2\mu_k\tau_d) \right] \right\}, \end{aligned} \quad (37a)$$

where  $\mu_k = \sqrt{\sigma_k^2 - \nu^2}$ . For FID, the corresponding expression is

$$\Psi_{FID}^{\tau_d} = \exp(-N\nu\tau_d) \prod_{k=1}^N \left\{ \cos(\mu_k\tau_d) + \frac{\nu}{\mu_k} \sin(\mu_k\tau_d) \right\}. \quad (37b)$$

From Eq. (36b) with  $\tau_{d1} = \tau_{d2} = \tau_d$  it follows that the dependence of the functional  $\Psi_{HE}^{\tau_d, \tau_d}$  on delay time  $\tau_d$  can be deduced from the dependence of the experimentally monitored FDMR response  $\Delta I_{HE}^\theta(\tau_d)$  on  $\tau_d$  at some fixed value of time  $\theta$ , e.g., at the maximum of the function  $\Theta(\theta)$ ,<sup>83</sup> which for the Pc+PT system occurs at  $\theta_{\max} \approx 60 \mu\text{s}$  with  $\Theta(\theta_{\max}) \approx 0.1244$ . This information can be obtained also from the number of fluorescence counts during some observation time  $t_{obs}$  after a MW pulse sequence, i.e., from the integral of the response over  $\theta$ :  $\overline{\Delta I_{HE}^{t_{obs}}}(\tau_d) = \int_0^{t_{obs}} d\theta \Delta I_{HE}^\theta(\tau_d) / t_{obs}$ .<sup>17</sup> The expression for  $\overline{\Delta I_{HE}^{t_{obs}}}(\tau_d)$  is the same as Eq. (36b) but with the function  $\Theta(\theta)$  replaced by  $\Theta^{t_{obs}}$   $= \int_0^{t_{obs}} d\theta \Theta(\theta) / t_{obs}$ . Curve 2 in Fig. 5 shows the function  $\Theta^{t_{obs}}$  for the Pc+PT system. At a typical experimental value  $t_{obs} = 1$  ms for the Pc+PT system<sup>14</sup> one gets  $\Theta^{t_{obs} = 1 \text{ ms}} = 0.0765$  and  $\Theta^{t_{obs} = 1 \text{ ms}} (\Delta^{(0)st} / \rho_{11}^{(0)st}) = 0.1175$ . At small delay time  $\tau_d \rightarrow 0$  when the HE MW pulse sequence  $\pi/2 - \tau_d - \pi - \tau_d - \pi/2$  approximates a  $2\pi$  pulse, the HE signal (36b) takes its minimal value  $\overline{\Delta I_{HE}^{t_{obs}}}(\tau_d \rightarrow 0) \rightarrow 0$ . Figure 6 shows the relative HE signal  $-\overline{\Delta I_{HE}^{t_{obs}}}(\tau_d)$  (curve 1) calculated with the exact equations (16a)–(16d) for a wide range of delay times  $\tau_d$  up to  $10^4 \mu\text{s}$  using the 1 RT model with  $\nu/2\pi = 30$  kHz,  $\sigma/2\pi = 85$  kHz, and  $t_{obs} = 1$  ms and for  $\pi/2$  MW pulses having pulse duration  $\tau_{\pi/2} = 30$  ps, such that  $\tau_{\pi/2}^{-1}$  is much greater than the width  $\Delta_0$  of the distribution  $P(\Delta)$ . For comparison we also show in the figure curve 2, which is the result of an analogous exact calculation with no jumps ( $\nu = 0$ ) and curve 3 obtained from analytical calculations of the FDMR HE signal using Eqs. (36b) and (37a) with appropriate parameter values for Pc+PT. A much slower decay of curve 2 at times of the order of a few microseconds demonstrates unambiguously the role of pure

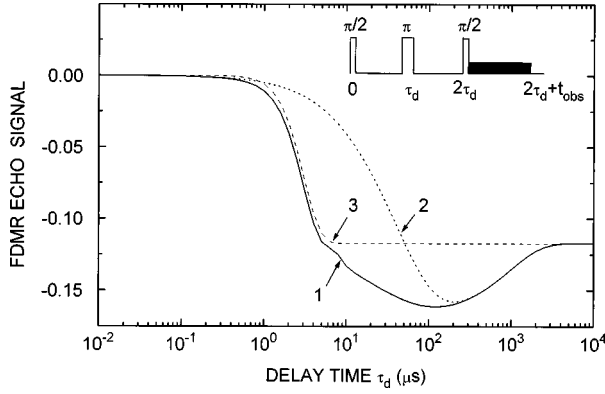


FIG. 6. Time dependence of the FDMR Hahn echo signal  $\overline{\Delta I}_{HE}^{obs}(\tau_d)$  on delay time  $\tau_d$  between exciting  $\pi/2$  and  $\pi$  pulses, calculated for the Pc+PT pair for short MW pulses ( $\tau_{\pi/2}=30$  ps) using the exact equations (16a)–(16d) for the 1 RT model with  $\sigma/2\pi=85$  kHz,  $\nu/2\pi=30$  kHz, curve 1, the exact equations (16a)–(16d) for the 1 RT model with  $\sigma/2\pi=85$  kHz,  $\nu=0$ , no jump case, curve 2, and analytical equations (36b) and (37a) with  $\sigma/2\pi=85$  kHz,  $\nu/2\pi=30$  kHz, curve 3. Fluorescence photon counting time  $t_{obs}=1$  ms.

dephasing for the system Pc+PT. Note also the very close behavior of curves 1 and 3 in this region. At times  $\tau_d \geq 10 \mu\text{s}$  the exact curve 1 shows a dip below analytical predictions which physically can be understood as originating from the depletion of fluorescing state 1 due to the ISC transitions  $1 \rightarrow X$ . Recall that the  $X$  substate population by this time is reduced (compared with its steady-state value with no MW field) as a result of the transfer of half its value to the long-lived substate  $Z$ . The subsequent growth of the HE signal at larger times ( $\tau_d \geq 200 \mu\text{s}$ ) is due to the ISC processes  $Z \rightarrow 0$ . Finally the limiting large-time value of the signal ( $\approx -0.1175$ ) corresponds to a reduction of the fluorescence intensity after the last  $\pi/2$  pulse only; all effects due to the first and second MW pulses have ceased at such times.

The analogous FDMR FID signal  $\overline{\Delta I}_{FID}^{obs}(\tau_d) = \int_0^{t_{obs}} d\theta \Delta I_{FID}^{\theta}(\tau_d)/t_{obs}$  calculated for the Pc+PT system using the exact equations (16a)–(16d) with very strong MW pulses ( $2W_{\pi/2} \gg \Delta_0$ ) is shown in Fig. 7 as curve 1. Dotted curve 3 in the figure was obtained from analytical calculations of the FDMR FID signal  $\overline{\Delta I}_{FID}^{obs}(\tau_d)$  using Eqs. (36a) and (37b) with  $\exp(-i\delta\tau_d)$  replaced by  $1/(1+\tau_d^2\Delta_0^2)$ . One can see that both signals drop rapidly on a time scale  $\tau_d \sim 10^{-2} - 10^{-1} \mu\text{s}$  determined by the inverse width  $\Delta_0 = 4.7$  MHz of the distribution  $P(\delta)$  ( $1/2\pi\Delta_0 \sim 0.03 \mu\text{s}$ ). The small-delay-time value of the signals  $\overline{\Delta I}_{FID}^{obs}(\tau_d \rightarrow 0) \rightarrow 2\Theta^{t_{obs}}(\Delta^{(0)st}/\rho_{11}^{(0)st}) \approx 0.235$  corresponds to the (1-ms-integrated) fluorescence reduction after a  $\pi$  pulse, which is the limit of FID MW pulse sequence  $\pi/2 - \tau_d - \pi/2$  as  $\tau_d \rightarrow 0$ . The long-delay-time value of the signals ( $\approx 0.1175$ ) is 2 times smaller and corresponds again to the situation when the molecule responds to the last  $\pi/2$  pulse only. The growth and subsequent decrease of the exactly calculated signal 1 near  $\tau_d \sim 200 \mu\text{s}$  results from intersystem crossings as in the case of the FDMR HE.

In experiments<sup>17</sup> on Pc+PT mixed crystals the MW field

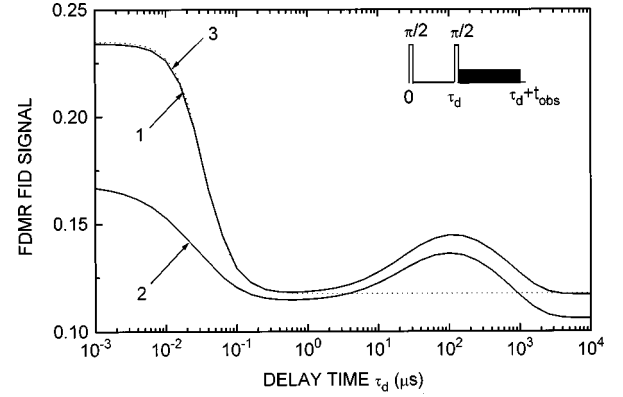


FIG. 7. Dependence of the FDMR FID signal  $\overline{\Delta I}_{FID}^{obs}(\tau_d)$  on delay time  $\tau_d$  between exciting  $\pi/2$  and probe  $\pi/2$  pulses, calculated for the Pc+PT pair using the exact equations (16a)–(16d) for the 1 RT model, curves 1 and 2, and analytical equations (36a) and (37b) with  $\sigma/2\pi=85$  kHz,  $\nu/2\pi=30$  kHz, curve 3. Curve 1 shows the signal for short MW pulses,  $\tau_{\pi/2}=30$  ps, while curve 2 corresponds to the experimental  $\pi/2$ -pulse duration,  $\tau_{\pi/2}=30$  ns (Ref. 17). Fluorescence photon counting time  $t_{obs}=1$  ms.

Rabi frequencies  $2W_{\pi/2}$  and  $2W_{\pi}$  were comparable with the width  $\Delta_0$  of the distribution  $P(\delta) = (1/\Delta_0)\exp(-\delta/\Delta_0)$  ( $2W_{\pi/2}/2\pi \approx 8.3$  MHz for an experimental  $\pi/2$  pulse duration of  $\tau_{\pi/2}=30$  ns). As a consequence, one cannot neglect the detuning  $\delta$  in calculating the molecular response to the  $\pi/2$  and  $\pi$  pulses. In this case Eq. (28) must be replaced by

$$G_{\pi/2} \approx \exp\{-i\pi[S_x + (c/s)S_z]/2\} = \exp\{-i\pi\Omega S'_z/4W\}, \quad (38a)$$

$$G_{\pi} \approx \exp\{-i\pi[S_x + (c/s)S_z]\} = \exp\{-i\pi\Omega S'_z/2W\} \quad (38b)$$

(recall that  $S'_z = cS_z + sS_x$ ,  $s = 2W/\Omega$ ,  $c = \delta/\Omega$ ), which can be calculated explicitly and used to obtain the responses (30a) and (30b) analytically. These expressions, however, are rather awkward and we do not quote them here. Note only that after numerical integration over  $\delta$  with distribution  $P(\delta)$  they predict the signals  $\overline{\Delta I}_{HE}^{obs}(\tau_d)$  and  $\overline{\Delta I}_{FID}^{obs}(\tau_d)$  to be similar in shapes to those shown in Figs. 6 and 7 as curves 3 but having slightly different values at small times. The exact calculations with Eqs. (16a)–(16d) confirm these conclusions. Figure 8 shows the dependence of the FDMR HE signal  $-\overline{\Delta I}_{HE}^{obs}(\tau_d)$  on delay time  $\tau_d$  calculated for the Pc+PT system using the experimental value<sup>17</sup> for the MW  $\pi/2$  pulse duration,  $\tau_{\pi/2}=30$  ns, ( $2W_{\pi/2} \leq \Delta_0$ ) and a 1 RT model with the same variance  $\sigma$  but different jump rates  $\nu$ . Note the limiting value  $-\overline{\Delta I}_{HE}^{obs}(\tau_d \rightarrow 0) \approx -0.032$  of the HE signal at  $2W_{\pi/2} \geq \Delta_0$  instead of zero in the case of  $2W_{\pi/2} \gg \Delta_0$ , Fig. 6. The analogous dependence for fixed jump rate  $\nu$  but different variances  $\sigma$  is shown in Fig. 9. Note that the oscillating behavior of the signal for large  $\sigma/2\nu$  is an artifact of the simplest 1 RT model. The effect of the number  $N$  of component RT processes in the model at fixed total variance  $\sigma = \sigma_k\sqrt{N}$  is demonstrated in Fig. 10 where two cases are shown corresponding to the ratios  $\sigma/2\nu \sim 1$  [Fig. 10(a)] and  $\sigma/2\nu \gg 1$  [Fig. 10(b)]. It follows from Fig. 10 that, when

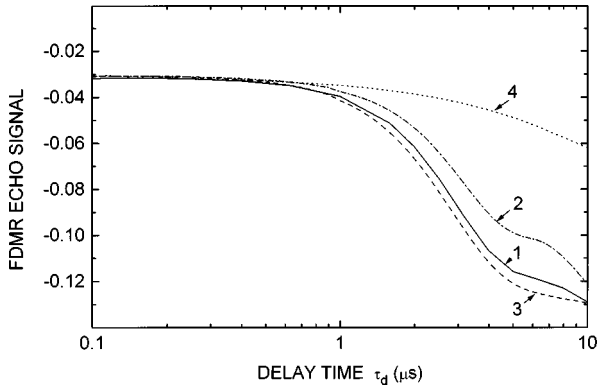


FIG. 8. FDMR Hahn echo signal  $-\overline{\Delta I_{HE}^{obs}}(\tau_d)$  calculated for the Pc+PT system using the experimental (Ref. 17)  $\pi/2$  pulse width,  $\tau_{\pi/2}=30$  ns, and using a 1 RT model with fixed variance  $\sigma/2\pi=85$  kHz and  $\nu/2\pi=30$  kHz, curve 1;  $\nu/2\pi=15$  kHz, curve 2;  $\nu/2\pi=50$  kHz, curve 3;  $\nu=0$ , curve 4. Fluorescence photon counting time  $t_{obs}=1$  ms.

$\sigma/2\nu \sim 1$ , a model with only very few RT processes is sufficient, while for  $\sigma/2\nu \gg 1$ , a larger number  $N$  of component processes is needed to provide convergent results. Finally, curve 2 in Fig. 7 shows the FDMR FID signal calculated for Pc+PT and a MW pulse Rabi frequency  $2W_{\pi/2} \leq \Delta_0$  corresponding to the pulse duration  $\tau_{\pi/2}=30$  ns used in the HE experiment.<sup>17</sup>

#### IV. CONCLUSIONS

Single-molecule spectroscopy combined with fluorescence-detected magnetic resonance (FDMR) techniques provides a sensitive method to study dynamical processes in a low-temperature host matrix which result in pure dephasing of the single triplet electron spin of a guest chromophore molecule in its triplet state. Typically this dynamics is slow and the conventional Bloch equations fail to describe experimental observations of various FDMR phenomena.

The stochastic theory of coherent FDMR phenomena developed in this article provides the basis for an appropriate description of both frequency- and time-domain FDMR phe-

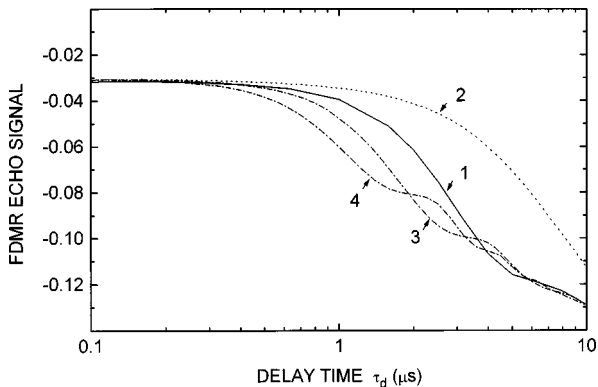


FIG. 9. FDMR Hahn echo signal  $-\overline{\Delta I_{HE}^{obs}}(\tau_d)$  calculated for the Pc+PT system using the experimental (Ref. 17)  $\pi/2$  pulse width,  $\tau_{\pi/2}=30$  ns, and using a 1 RT model with fixed jump rate  $\nu/2\pi=30$  kHz and  $\sigma/2\pi=85$  kHz, curve 1;  $\sigma/2\pi=30$  kHz, curve 2;  $\sigma/2\pi=150$  kHz, curve 3;  $\sigma/2\pi=250$  kHz, curve 4. Fluorescence photon counting time  $t_{obs}=1$  ms.

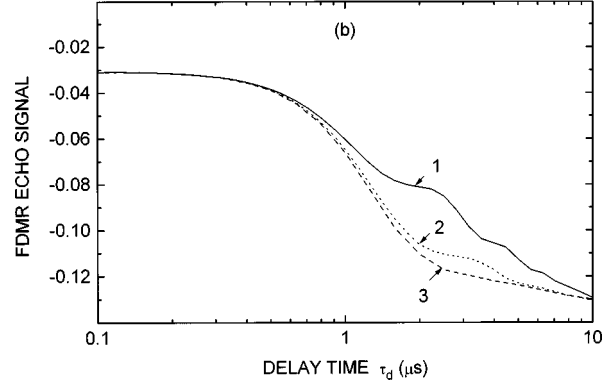
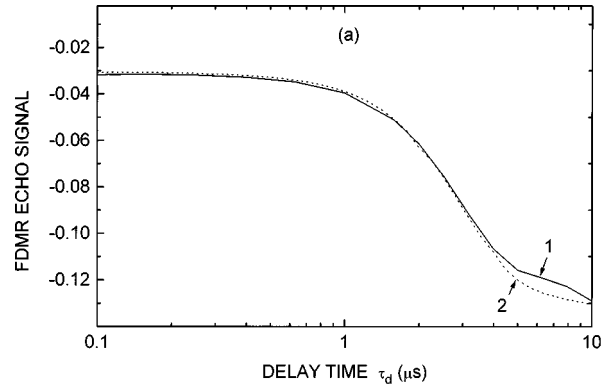


FIG. 10. Dependences of calculated FDMR Hahn echo signal  $-\overline{\Delta I_{HE}^{obs}}(\tau_d)$  on number  $N$  of component processes in the model: (a)  $N$  RT model calculations for Pc+PT system with  $\pi/2$  pulse width  $\tau_{\pi/2}=30$  ns,  $\nu/2\pi=30$  kHz,  $\sigma/2\pi=85$  kHz,  $\sigma_k=\sigma/\sqrt{N}$  with  $N=1$  (curve 1),  $N=2$  (curve 2), and (b)  $N$  RT model calculations for Pc+PT system at  $\pi/2$  pulse width  $\tau_{\pi/2}=30$  ns,  $\nu/2\pi=30$  kHz,  $\sigma/2\pi=250$  kHz,  $\sigma_k=\sigma/\sqrt{N}$  with  $N=1$  (curve 1),  $N=2$  (curve 2), and  $N=3$  (curve 3).

nomena. Owing to the long-time scales of the experiments, a density matrix approach can be used since the time averaging for a single molecule is equivalent to an ensemble average over the stochastic parameters in the problem. A physically adequate model of  $N$  independent random telegraph processes for dephasing fluctuations  $U^t$  of the triplet spin frequency allows one to construct an exact set of equations for the density matrix averaged over fluctuation histories  $U^t$ . The equations incorporate the non-Markovian effects of MW-field-dependent dephasing. Using them one can calculate cw-transient FDMR responses of a molecule to a MW field in cases of both fast and slow fluctuations  $U^t$ .

The general theory has been applied to calculate (i) the FDMR line shape, (ii) the FDMR free induction decay, and (iii) the FDMR Hahn echo for single pentacene molecules in crystalline *p*-terphenyl. Three causes of broadening in the FDMR line shape and decay in the FDMR FID and FDMR HE signals are (i) the spin resonance frequency distribution owing to different pentacene proton spin configurations, (ii) the pure dephasing of triplet spin substates due to the spin frequency fluctuations  $U^t$  *p*-terphenyl proton spin flip-flops, and (iii) the triplet sublevel lifetimes. The FDMR line shape is determined by the first mechanism at low MW intensity, by the second mechanism at moderate MW field power due to additional saturation broadening, and by the third mechanism at high MW intensity owing to the suppression of pure

dephasing by the MW field. The best fit calculations of FDMR line shapes with  $\nu/2\pi=30$  kHz and  $\sigma/2\pi=85$  kHz are in excellent agreement with experimental observations at low, medium, and high MW powers as distinct from the Bloch equations which predict much wider FDMR line shapes. The FDMR FID rate is determined mainly by the spin resonance frequency distribution while the FDMR HE signal by the pure dephasing. In the case of slow fluctuations,  $\sigma \gg \nu$ , the FDMR HE decay is nonexponential.

It should be noted that our calculations as applied to Pc +PT are approximate since no complete experimental study of different FDMR phenomena has ever been carried out on the *same* molecule. On the contrary, different phenomena have been studied for different single molecules with variations of relevant parameters from molecule to molecule. In principle, our theory makes it possible to calculate the molecular response for a variety of FDMR phenomena for the same single molecule, allowing one to extract complementary information on the molecule, the host, and the molecule-host interaction.

### ACKNOWLEDGMENTS

The investigations were supported by the National Science Foundation under Grant No. PHY-9414515 and Volkswagenstiftung under Grant No. I/72171. Partial support from the Belarus Foundation for Fundamental Research under Grant No F96-117 is also acknowledged.

### APPENDIX

In this appendix we present the details of a procedure that enables us to average the linear stochastic matrix equations (1) over histories of the multiplicative fluctuations  $U^t$  modeled by an  $N$  RT Markov jump process. We deduce here Eqs. (16a)–(16d) and, as well, discuss the derivation of more conventional equations for so-called “marginal” averages which are completely equivalent to Eqs. (16a)–(16d). First, we recall some known results concerning the application of the differentiation formulas approach (see, e.g., Refs. 65 and 73) to average a stochastic equation of the form  $\dot{x}^t = Ax^t + B\xi^t x^t + x_0$ , where  $A$  and  $B$  are time-independent matrices,  $x_0$  is a nonstochastic vector, and  $\xi^t$  is a stochastic Markov-type process. Averaging of this equation over the process  $\xi^t$  realizations leads to the equation

$$d\langle x^t \rangle / dt = A\langle x^t \rangle + B\langle \xi^t x^t \rangle + x_0, \quad (\text{A1})$$

where the new average  $\langle \xi^t x^t \rangle$  now appears. Differentiation formulas provide a way to calculate this last average. In general, these are the equations

$$d\langle F(t, \xi^t) \Psi[\xi^t] \rangle / dt = \partial \langle F(t, \xi^t) \Psi[\xi^t] \rangle / \partial t + \langle \{L_\xi^+ F(t, \xi^t)\} \Psi[\xi^t] \rangle \quad (\text{A2})$$

for the product averages  $\langle F(t, \xi^t) \Psi[\xi^t] \rangle$ , where  $F(t, \xi^t)$  is an arbitrary function of time  $t$  and of the process  $\xi^t$ ,  $\Psi[\xi^t]$  is a functional of the process  $\xi^t$ , and  $\partial/\partial t$  means differentiation over  $t$  at constant  $\xi^t$ . The (linear) operator  $L_\xi^+$  acts on the function  $F(t, \xi^t)$  only and is the Hermitian conjugate of the generating operator  $L_\xi$  of the process  $\xi^t$ , i.e., of the operator which governs the time evolution of the conditional

probability density  $p(\xi, t | \xi', t')$  for the process  $\xi^t$  to take the value  $\xi$  at time  $t$  provided that at previous time  $t'$  it took the value  $\xi'$  according to the “forward” equation  $\partial p(\xi, t | \xi', t') / \partial t = L_\xi p(\xi, t | \xi', t')$ . Note that the operator  $L_\xi^+$  enters the “backward” equation  $\partial p(\xi, t | \xi', t') / \partial t' = -L_\xi^+ p(\xi, t | \xi', t')$ . Below we deal with cases when  $F(t, \xi^t)$  does not depend explicitly on time  $t$  [ $F(t, \xi^t) = F(\xi^t)$ ] and  $\partial \langle F(t, \xi^t) \Psi[\xi^t] \rangle / \partial t = \langle F(t, \xi^t) \dot{\Psi}[\xi^t] \rangle$  with  $\dot{\Psi}[\xi^t]$  equal to the right-hand side of the corresponding stochastic differential equation satisfied by  $\Psi[\xi^t]$  [i.e., of Eq. (A1) with  $\Psi[\xi^t] = x^t$ ]. When  $\xi^t$  is a symmetric RT process, having jump rate  $\nu$  between two possible values  $\pm\sigma$ , the conditional probability density  $p(\xi, t | \xi', t')$  depends on the difference  $\tau = t - t'$  only, the operators  $L_\xi, L_\xi^+$  coincide and act according to  $L_\xi F(\xi) = -\nu[F(\xi) - F(-\xi)]$ , and the differentiation formula for  $\langle \xi^t x^t \rangle$  reads

$$d\langle \xi^t x^t \rangle / dt = \langle \xi^t \dot{x}^t \rangle - 2\nu \langle \xi^t x^t \rangle = (A - 2\nu I) \langle \xi^t x^t \rangle + \sigma^2 B \langle x^t \rangle, \quad (\text{A3})$$

where  $I$  is the unit matrix and we use the obvious relation  $(\xi^t)^2 = \sigma^2$ . Equations (A3) and (A1) provide a closed set of equations for exact calculation of the average  $\langle x^t \rangle$  in the case of a symmetric RT process  $\xi^t$ . The generalization to the case of a nonsymmetric RT process which performs jumps between values  $\xi_1$  and  $\xi_2$  with probabilities  $\varphi_{1 \rightarrow 2} = \nu$  and  $\varphi_{2 \rightarrow 1} = \mu$  is straightforward and involves the use of more complicated differentiation formulas [Ref. 65, p. 134, Eq. (3.53'')]

$$d\langle \xi^t x^t \rangle / dt = \{A + (\xi_1 + \xi_2)B - (\nu + \mu)I\} \langle \xi^t x^t \rangle + \{(\nu\xi_2 + \mu\xi_1)I - \xi_1\xi_2 B\} \langle x^t \rangle \quad (\text{A4})$$

instead of Eq. (A3).

Now we construct the analogous closed set of equations for Eq. (1) with  $N$  symmetric RT fluctuations  $U^t = \sum_{k=1}^N U_k^t$ . Equation (A1) coincides with Eq. (16a). To deduce the equations for averages  $R^{\{k\}t} = \langle U_k^t r^t \rangle$  we note that this average can be written as  $R^{\{k\}t} = \langle U_k^t R^{\{-k\}t} \rangle_{(k)}$ , where  $\langle \dots \rangle_{(k)}$  implies an average over the process  $U_k^t$  only and  $R^{\{-k\}t} = \langle r^t \rangle_{(1, \dots, k-1, k+1, \dots, N)}$  is still a stochastic vector (with respect to the  $k$ th process) resulting from partial averaging of the vector  $r^t$  over histories of all component processes excluding the  $k$ th process. Therefore, one can apply the differentiation formula (A3) to Eq. (1) and get

$$dR^{\{k\}t} / dt = -2\nu R^{\{k\}t} - \langle U_k^t \dot{R}^{\{-k\}t} \rangle_{(k)} \quad (\text{A5})$$

$$= -2\nu R^{\{k\}t} + \left\langle U_k^t \left[ DR^{\{-k\}t} - iF \sum_l^N \langle U_l^t r^t \rangle_{(1, \dots, k-1, k+1, \dots, N)} + r_0 \right] \right\rangle_{(k)} \\ = (D - 2\nu I) R^{\{k\}t} - iF \sigma_k^2 R^t - iF \sum_{l \neq k}^N R^{\{k, l\}t}, \quad (\text{A6})$$

i.e., Eq. (16b). The procedure to deduce the next equation (16c) is more time consuming but straightforward. One can represent the averages in Eq. (A5) in the form  $R^{\{k, l\}t}$

$= \langle U_k^t \langle U_l^t R^{(-k, -l)t} \rangle_{(l)(k)} \rangle$  and then, considering the averages  $\langle U_l^t R^{(-k, -l)t} \rangle_{(l)}$  as functionals  $\Phi_l[U_k^t]$  of the process  $U_k^t$  satisfying the differentiation formulas

$$\begin{aligned} \Phi_l[U_k^t] &= -2\nu \Phi_l[U_k^t] + \langle U_l^t R^{(-k, -l)t} \rangle_{(l)} \\ &= (D - 2\nu I) \Phi_l[U_k^t] - iF \sum_{m \neq k}^N \langle U_m^t \Phi_l[U_k^t] \rangle_{(m)} \\ &\quad - iF \langle U_k^t U_l^t R^{(-l)t} \rangle_{(l)} - iF \sigma_k^2 R^{(-k)t}, \end{aligned}$$

one can substitute this equation into the differentiation formulas for the average  $\langle U_k^t \Phi_l[U_k^t] \rangle_{(k)}$ :

$$\begin{aligned} dR^{(k, l)t}/dt &= d \langle U_k^t \Phi_l[U_k^t] \rangle_{(k)} / dt \\ &= -2\nu \langle U_k^t \Phi_l[U_k^t] \rangle_{(k)} + \langle U_k^t \dot{\Phi}_l[U_k^t] \rangle_{(k)} \\ &= (D - 4\nu I) R^{(k, l)t} - iF \sum_{m \neq k, l}^N R^{(k, l, m)t} \\ &\quad - iF \sigma_l^2 R^{(k)t} - iF \sigma_k^2 R^{(l)t}, \end{aligned} \quad (A7)$$

where  $R^{(k, l, m)t} = \langle U_k^t U_m^t \Phi_l[U_k^t] \rangle_{(k, m)} = \langle U_k^t U_l^t U_m^t r^t \rangle$ . Analogously, using the differentiation formula (A3) repeatedly, one can construct the other equations (16c)–(16d). The explicit form of Eqs. (16a)–(16d) for the model of 2 RT processes, written in block-matrix form, is

$$\begin{aligned} d\mathbf{R}^t/dt &= \begin{pmatrix} D & -iF & -iF & 0 \\ -iF\sigma_1^2 & D - 2\nu I & 0 & -iF \\ -iF\sigma_2^2 & 0 & D - 2\nu I & -iF \\ 0 & -iF\sigma_2^2 & -iF\sigma_1^2 & D - 4\nu I \end{pmatrix} \mathbf{R}^t \\ &\quad + \mathbf{R}_0, \end{aligned} \quad (A8)$$

where  $\mathbf{R}_i^t = R^t$ ,  $R^{\{1\}t}$ ,  $R^{\{2\}t}$ ,  $R^{\{1,2\}t}$ , and  $\mathbf{R}_{0i} = r_0, Z_{1,8}, Z_{1,8}, Z_{1,8}$ .

For Markov jump fluctuations, there exists another, more conventional and completely equivalent, method (see, e.g., Refs. 24,32,34,74,75,85,65,76,77, and 84 for reviews) to construct an *exact* closed set of equations for partially averaged quantities  $R^{[\lambda_1, \dots, \lambda_N]t}$ , so-called ‘‘end marginal’’ averages, which are the partial averages of the vector  $r^t$  over only those histories of all component processes  $U_k^t$  which end at time  $t$  with some specific value  $U_k = \lambda_k \sigma_k$ , where  $\lambda_k = \text{sgn}(U_k)$ . In fact, one can consider the  $N$  RT process  $U^t = \sum_{k=1}^N U_k^t$  as a Markov jump process with possible values  $U_{[\lambda_1, \dots, \lambda_N]} = \sum_k \lambda_k \sigma_k$  corresponding to different configurations of  $N$ -component RT processes, taking at the moment  $t$  the values  $U_k = \lambda_k \sigma_k$  with  $\lambda_k = \pm$  depending on whether the  $k$ th RT process is in the state  $U_k = +\sigma_k$  or in the state  $U_k = -\sigma_k$ . The total process  $U^t$  jumps between these values with rate  $\nu$ . For example, state  $U_{[\lambda_1, \dots, \lambda_N]}$  can jump to another possible state  $U_{[\lambda'_1, \dots, \lambda'_N]}$  in which only one  $\lambda_k$  from the combination  $\lambda_1, \dots, \lambda_N$  is changed in sign (we neglect the possibility for simultaneous jumps of few-

component processes). Since the component RT processes are assumed to be independent, the conditional probability density  $p(\lambda_1, \dots, \lambda_N, t | \lambda'_1, \dots, \lambda'_N, t')$  to find the process  $U^t$  in the state  $U_{[\lambda_1, \dots, \lambda_N]}$  at time  $t$  provided that at time  $t' \leq t$  it was in the state  $U_{[\lambda'_1, \dots, \lambda'_N]}$  can be factorized,  $p(\lambda_1, \dots, \lambda_N, t | \lambda'_1, \dots, \lambda'_N, t') = \prod_k p_k(\lambda_k, t | \lambda'_k, t')$ , as a product of component RT conditional probability densities  $p_k(\lambda_k, t | \lambda'_k, t')$ . Thus, the ‘‘forward’’ equation for  $p(\lambda_1, \dots, \lambda_N, t | \lambda'_1, \dots, \lambda'_N, t')$  is of the form

$$\begin{aligned} dp(\lambda_1, \dots, \lambda_N, t | \lambda'_1, \dots, \lambda'_N, t')/dt &= L_{[\lambda_1, \dots, \lambda_N]} p(\lambda_1, \dots, \lambda_N, t | \lambda'_1, \dots, \lambda'_N, t') \\ &= -N\nu p(\lambda_1, \dots, \lambda_N, t | \lambda'_1, \dots, \lambda'_N, t') \\ &\quad + \nu \sum_k p_k(-\lambda_k, t | \lambda'_k, t') \prod_{l \neq k} p_l(\lambda_l, t | \lambda'_l, t'), \end{aligned} \quad (A9)$$

where  $L_{[\lambda_1, \dots, \lambda_N]}$  is the generating operator defined by the second row of Eq. (A9). Now we can write the equations for ‘‘end marginal’’ averages  $R^{[\lambda_1, \dots, \lambda_N]t}$  as

$$\begin{aligned} dR^{[\lambda_1, \dots, \lambda_N]t}/dt &= (D - iF U_{[\lambda_1, \dots, \lambda_N]} + L_{[\lambda_k]}) R^{[\lambda_1, \dots, \lambda_N]t} + r_0/2^N \\ &= (D - iF U_{[\lambda_1, \dots, \lambda_N]} - N\nu) R^{[\lambda_1, \dots, \lambda_N]t} \\ &\quad + \nu \sum_k R^{[\lambda_1, \dots, \lambda_{k-1}, \lambda_{k+1}, \dots, \lambda_N]t} + r_0/2^N. \end{aligned} \quad (A10)$$

The completely averaged vector  $R^t$  is obtained by summation of all ‘‘end marginally’’ averaged vectors  $R^t = \sum R^{[\lambda_1, \dots, \lambda_N]t}$ . To compare with Eq. (A4), let us write explicitly Eq. (A10) for the case of a 2 RT process. In block matrix form for the vector  $\bar{\mathbf{R}}^t$  with components  $\bar{\mathbf{R}}_i^t = R^{[-, -]t}, R^{[+, -]t}, R^{[-, +]t}, R^{[+, +]t}$  the latter are

$$\begin{aligned} d\bar{\mathbf{R}}^t/dt &= \begin{pmatrix} D_{--} & \nu I & \nu I & 0 \\ \nu I & D_{+-} & 0 & \nu I \\ \nu I & 0 & D_{-+} & \nu I \\ 0 & \nu I & \nu I & D_{++} \end{pmatrix} \bar{\mathbf{R}}^t + \bar{\mathbf{R}}_0, \end{aligned} \quad (A11)$$

where  $D_{\lambda_1 \lambda_2} = D - iF(\lambda_1 \sigma_1 + \lambda_2 \sigma_2) - 2\nu I$  and  $\bar{\mathbf{R}}_{0i} = r_0/4, r_0/4, r_0/4, r_0/4$ . It follows from the definitions (2)–(5) and (6) of matrices  $D$  and  $F$  that the matrices in Eqs. (A11) are just the matrix  $D$  with MW detuning  $\delta$  replaced by  $\delta + U_{[\lambda_1, \dots, \lambda_N]}$ . Zeros on the secondary diagonals of the matrix in Eq. (A11) result from the absence of simultaneous jumps of both component processes  $U_1^t$  and  $U_2^t$ . One can show straightforwardly that Eqs. (A8) and Eqs. (A11) result in the same solutions both in steady-state and transient cases.

- <sup>1</sup>W. E. Moerner and L. Kador, *Phys. Rev. Lett.* **62**, 2535 (1989).
- <sup>2</sup>M. Orrit and J. Bernard, *Phys. Rev. Lett.* **65**, 2716 (1990).
- <sup>3</sup>W. E. Moerner and W. E. Ambrose, *Phys. Rev. Lett.* **66**, 1376 (1991).
- <sup>4</sup>W. P. Ambrose and W. E. Moerner, *Nature (London)* **349**, 225 (1991).
- <sup>5</sup>W. P. Ambrose, Th. Basché, and W. E. Moerner, *J. Chem. Phys.* **95**, 7150 (1991).
- <sup>6</sup>A. Zumbusch, L. Fleury, R. Brown, J. Bernard, and M. Orrit, *Phys. Rev. Lett.* **70**, 3584 (1993).
- <sup>7</sup>J. Bernard, L. Fleury, H. Talon, and M. Orrit, *J. Chem. Phys.* **98**, 850 (1993).
- <sup>8</sup>Th. Basché, W. E. Moerner, M. Orrit, and H. Talon, *Phys. Rev. Lett.* **69**, 1516 (1992).
- <sup>9</sup>W. E. Moerner and T. Basché, *Angew. Chem. Int. Ed. Engl.* **32**, 457 (1993).
- <sup>10</sup>M. Orrit, J. Bernard, and R. I. Personov, *J. Phys. Chem.* **97**, 10 256 (1993).
- <sup>11</sup>*Single-Molecule Optical Detection, Imaging and Spectroscopy*, edited by T. Basché, W. E. Moerner, M. Orrit, and U. P. Wild (VCH, Weinheim, 1997).
- <sup>12</sup>J. Köhler, J. A. J. M. Disselhorst, M. C. J. M. Donckers, E. J. J. Groenen, J. Schmidt, and W. E. Moerner, *Nature (London)* **363**, 242 (1993).
- <sup>13</sup>J. Wrachtrup, C. von Borczyskowski, J. Bernard, M. Orrit, and R. Brown, *Nature (London)* **363**, 244 (1993).
- <sup>14</sup>J. Wrachtrup, C. von Borczyskowski, J. Bernard, M. Orrit, and R. Brown, *Phys. Rev. Lett.* **71**, 3565 (1993).
- <sup>15</sup>R. Brown, J. Wrachtrup, M. Orrit, J. Bernard, and C. von Borczyskowski, *J. Chem. Phys.* **100**, 7182 (1994).
- <sup>16</sup>J. Köhler, A. C. J. Brouwer, E. J. J. Groenen, and J. Schmidt, *Chem. Phys. Lett.* **228**, 47 (1994).
- <sup>17</sup>J. Wrachtrup, C. von Borczyskowski, J. Bernard, R. Brown, and M. Orrit, *Chem. Phys. Lett.* **245**, 262 (1995).
- <sup>18</sup>J. Wrachtrup and C. von Borczyskowski, *J. Lumin.* **64**, 13 (1995).
- <sup>19</sup>A. Gruber, M. Vogel, J. Schuster, J. Wrachtrup, and C. von Borczyskowski, *Exp. Tech. Phys. (Lemgo, Ger.)* **42**, 219 (1995).
- <sup>20</sup>J. Köhler, A. C. J. Brouwer, E. J. J. Groenen, and J. Schmidt, *Science* **268**, 1457 (1995).
- <sup>21</sup>J. Köhler, A. C. J. Brouwer, E. J. J. Groenen, and J. Schmidt, *Chem. Phys. Lett.* **250**, 137 (1996).
- <sup>22</sup>A. C. J. Brouwer, J. Köhler, E. J. J. Groenen, and J. Schmidt, *J. Chem. Phys.* **105**, 2212 (1996).
- <sup>23</sup>A. G. Redfield, *Phys. Rev.* **98**, 1787 (1955).
- <sup>24</sup>A. Abragam, *The Principles of Nuclear Magnetism* (Clarendon, Oxford, 1970).
- <sup>25</sup>A. N. Argyres and P. L. Kelley, *Phys. Rev.* **134**, A98 (1964).
- <sup>26</sup>C. A. Van 't Hof and J. Schmidt, *Mol. Phys.* **38**, 309 (1979).
- <sup>27</sup>R. Kubo, in *Fluctuation, Relaxation and Resonance in Magnetic Systems*, edited by D. Ter Haar (Oliver and Boyd, Edinburgh, 1961), p. 23; *Adv. Chem. Phys.* **15**, 101 (1969); *J. Phys. Soc. Jpn.* **26**, 1 (1969); J. H. Freed, G. V. Bruno, and C. F. Polnaszek, *J. Phys. Chem.* **75**, 3385 (1971).
- <sup>28</sup>P. R. Berman and R. G. Brewer, *Phys. Rev. A* **32**, 2784 (1985).
- <sup>29</sup>S. Ya. Kilin and A. P. Nizovtsev, *J. Phys. B* **19**, 3457 (1986).
- <sup>30</sup>P. A. Apanasevich, S. Ya. Kilin, and A. P. Nizovtsev, *Zh. Prikl. Spektrosk.* **47**, 887 (1987) [*J. Appl. Spectrosc.* **47**, 1213 (1988)].
- <sup>31</sup>S. Ya. Kilin and A. P. Nizovtsev, *Phys. Rev. A* **42**, 4403 (1990).
- <sup>32</sup>A. I. Burshtein, A. A. Zharikov, and S. I. Temkin, *J. Phys. B* **21**, 1907 (1988).
- <sup>33</sup>A. I. Burshtein and V. S. Malinovsky, *J. Opt. Soc. Am. B* **8**, 1098 (1991).
- <sup>34</sup>A. I. Burshtein, A. A. Zharikov, and V. S. Malinovsky, *Phys. Rev. A* **43**, 1538 (1991).
- <sup>35</sup>E. Geva, R. Kosloff, and J. L. Skinner, *J. Chem. Phys.* **102**, 8541 (1995).
- <sup>36</sup>W. G. Breiland, H. C. Brenner, and C. B. Harris, *J. Chem. Phys.* **62**, 3458 (1975).
- <sup>37</sup>C. B. Harris and W. G. Breiland, in *Laser and Coherence Spectroscopy*, edited by J. I. Steinfeld (Plenum, New York, 1978), p. 373.
- <sup>38</sup>M. Glasbeek and R. Hond, *Phys. Rev. B* **23**, 4220 (1981).
- <sup>39</sup>H. C. Brenner, in *Triplet State ODMR Spectroscopy*, edited by R. H. Clarke (Wiley, New York, 1982), p. 185.
- <sup>40</sup>S. Ya. Kilin, A. P. Nizovtsev, P. R. Berman, J. Wrachtrup, and C. von Borczyskowski, *J. Lumin.* **72-74**, 1013 (1997).
- <sup>41</sup>S. Ya. Kilin, A. P. Nizovtsev, P. R. Berman, J. Wrachtrup, and C. von Borczyskowski, *Phys. Rev. B* **56**, 24 (1997).
- <sup>42</sup>S. Ya. Kilin, A. P. Nizovtsev, P. R. Berman, C. von Borczyskowski, and J. Wrachtrup, *Opt. Spectrosc.* **82**, 1010 (1997) [*Opt. Spectrosc.* **82**, 927 (1997)].
- <sup>43</sup>S. P. McGlynn, T. Azumi, and M. Kinoshita, *Molecular Spectroscopy of the Triplet State* (Prentice Hall, Englewood Cliffs, NJ, 1969).
- <sup>44</sup>Th. Basché, W. P. Ambrose, and W. E. Moerner, *J. Opt. Soc. Am. B* **9**, 829 (1992).
- <sup>45</sup>T. Basché and W. E. Moerner, *Nature (London)* **355**, 335 (1992).
- <sup>46</sup>M. Orrit, J. Bernard, A. Zumbusch, and R. I. Personov, *Chem. Phys. Lett.* **196**, 595 (1992); **199**, 408 (1992).
- <sup>47</sup>L. Fleury, A. Zumbusch, M. Orrit, R. Brown, and J. Bernard, *J. Lumin.* **56**, 15 (1993).
- <sup>48</sup>P. D. Reilly and J. L. Skinner, *Phys. Rev. Lett.* **71**, 4257 (1993); *J. Chem. Phys.* **101**, 959 (1994); **101**, 965 (1994); **102**, 1540 (1995).
- <sup>49</sup>G. Zumofen and J. Klafter, *Chem. Phys. Lett.* **219**, 303 (1994).
- <sup>50</sup>T. E. Orlowski and A. H. Zewail, *J. Chem. Phys.* **70**, 1390 (1979).
- <sup>51</sup>V. Lawetz, G. Orlandi, and W. Siebrand, *J. Chem. Phys.* **56**, 4058 (1972).
- <sup>52</sup>M. O. Srinivas and E. B. Davies, *Opt. Acta* **28**, 981 (1981); S. Ya. Kilin, *Quantum Optics: Fields and their Detection* (Nauka i Technika, Minsk, 1990); H. J. Carmichael, *An Open System Approach to Quantum Optics*, Lecture Notes in Physics, Vol. 18 (Springer-Verlag, Berlin, 1993).
- <sup>53</sup>S. Ya. Kilin, T. M. Maevskaya, A. P. Nizovtsev, V. N. Shatokhin, P. R. Berman, C. von Borczyskowski, J. Wrachtrup, and L. Fleury, *J. Lumin.* **76&77**, 288 (1998); *Phys. Rev. A* **57**, 1400 (1998).
- <sup>54</sup>C. A. Hutchinson, J. H. Nicholas, and G. W. Scott, *J. Chem. Phys.* **53**, 1906 (1970).
- <sup>55</sup>L. Allen and J. H. Eberly, *Optical Resonance and Two-Level Atoms* (Wiley, New York, 1975).
- <sup>56</sup>A. Szöke, *Opt. Lett.* **2**, 36 (1978).
- <sup>57</sup>A. M. Bonch-Bruевич, T. A. Vartanyan, and V. V. Khromov, *Zh. Éksp. Teor. Fiz.* **78**, 538 (1980) [*Sov. Phys. JETP* **51**, 271 (1980)].
- <sup>58</sup>R. G. DeVoe and R. G. Brewer, *Phys. Rev. Lett.* **50**, 1269 (1983).
- <sup>59</sup>T. Muramoto and A. Szabo, *Phys. Rev. A* **38**, 5928 (1988).
- <sup>60</sup>A. Szabo and R. Kaarli, *Phys. Rev. B* **44**, 12 307 (1991).
- <sup>61</sup>C. B. Harris, R. L. Schlupp, and H. Schuch, *Phys. Rev. Lett.* **30**, 1019 (1973).

- <sup>62</sup>R. H. Feynman, F. L. Vernon, Jr., and R. W. Hellwarth, *J. Appl. Phys.* **28**, 49 (1957).
- <sup>63</sup>D. A. Warshalovich, A. N. Moskalev, and V. K. Khersonskii, *Quantum Theory of the Angular Momentum* (Nauka, Leningrad, 1975).
- <sup>64</sup>A. Brissaud and U. Frisch, *J. Math. Phys.* **10**, 524 (1974).
- <sup>65</sup>V. I. Klyatskin, *Stochastic Equations and Waves in Random Media* (Nauka, Moscow, 1980).
- <sup>66</sup>K. Wódkiewicz and J. H. Eberly, *Phys. Rev. A* **32**, 992 (1985).
- <sup>67</sup>V. S. Malinovsky, *Phys. Rev. A* **52**, 4921 (1995).
- <sup>68</sup>K. Wódkiewicz, B. W. Shore, and J. H. Eberly, *J. Opt. Soc. Am. B* **1**, 398 (1984).
- <sup>69</sup>A. I. Burshtein and B. I. Yakobson, *Khim. Fiz.* **1**, 479 (1982).
- <sup>70</sup>J. R. Klauder and P. W. Anderson, *Phys. Rev.* **125**, 912 (1962).
- <sup>71</sup>P. Hu and S. R. Hartmann, *Phys. Rev. B* **9**, 1 (1974).
- <sup>72</sup>P. Hu and L. R. Walker, *Phys. Rev. B* **18**, 1300 (1978).
- <sup>73</sup>V. M. Loginov and V. E. Shapiro, *Dynamical Systems under the Stochastic Interactions* (Nauka, Novosibirsk, 1983).
- <sup>74</sup>A. I. Burshtein, *Zh. Eksp. Teor. Fiz.* **48**, 85 (1965) [*Sov. Phys. JETP* **21**, 567 (1965)].
- <sup>75</sup>A. I. Burshtein, *Lectures on Quantum Kinetics* (Izd. NGU, Novosibirsk, 1968).
- <sup>76</sup>B. Shore, *J. Opt. Soc. Am. B* **1**, 176 (1984).
- <sup>77</sup>B. W. Shore, *The Theory of Coherent Atomic Excitation* (Wiley, New York, 1990), Vol. 2.
- <sup>78</sup>E. G. Pestov and S. G. Rautian, *Zh. Eksp. Teor. Fiz.* **64**, 2032 (1973) [*Sov. Phys. JETP* **37**, 1025 (1973)].
- <sup>79</sup>M. Goldman, *Spin Temperature and Nuclear Magnetic Resonance in Solids* (Oxford University Press, Oxford, 1970).
- <sup>80</sup>J. Schmidt and J. H. van der Waals, in *Time Domain Electron Spin Resonance*, edited by L. Kevan and R. N. Shwartz (Wiley, New York, 1972), p. 343.
- <sup>81</sup>T. S. T. Lin, J. L. Ong, D. J. Sloop, and H. L. Yu, in *Pulsed EPR: A New Field of Application*, edited by C. P. Kreijers, E. J. Reijerse, and J. Schmidt (North-Holland, Amsterdam, 1988), p. 191.
- <sup>82</sup>A. J. van Strien and J. Schmidt, *Chem. Phys. Lett.* **70**, 513 (1980).
- <sup>83</sup>J. Wrachtrup, Ph.D. thesis, Free University, Berlin, 1994.
- <sup>84</sup>K. M. Salikhov, A. G. Semenov, and Y. D. Tsvetkov, in *Electron Spin Echo and Its Applications*, edited by Y. N. Molin (Nauka, Novosibirsk, 1976).
- <sup>85</sup>N. N. Korst, *Teor. Mat. Fiz.* **6**, 265 (1971).